Food Chemistry: X 35 (2026) 103808

Contents lists available at ScienceDirect

Food Chemistry: X

journal homepage: www.sciencedirect.com/journal/food-chemistry-x

Multi-omics integrated analysis of the secondary metabolic regulatory network in *Aquilaria sinensis* leaves and the mechanism of its enhanced antioxidant function

Zixiao Jiang [a], Haoji Liang [a], Dandan Chen [a], Yaohua Huang [b], Nie Li [b], Yiqi Wang [c], Yangyang Liu [a,*]

[a] *Hainan Provincial Key Laboratory of Resources Conservation and Development of Southern Medicine, Key Laboratory of State Administration of Traditional Chinese Medicine for Agarwood Sustainable Utilization, International Joint Research Center for Quality of Traditional Chinese Medicine, Hainan Branch of Institute of Medicinal Plant Development, Chinese Academy of Medical Sciences, Peking Union Medical College, Haikou 570311, China*

[b] *Guangdong Qinanxiang Biological Research Co., Ltd., Chaozhou 521051, China*

[c] *Baoting Li and Miao Autonomous County Hospital of Traditional Chinese Medicine, Baoting 572300, China*

ARTICLE INFO

Keywords:
Aquilaria sinensis leaf
Proteomics
Metabolomics
Secondary metabolites
Antioxidant activities

ABSTRACT

Aquilaria sinensis leaves are rich in bioactive compounds and have attracted increasing attention for their potential use in functional foods and health products. However, the effects of different processing methods on their metabolite profiles, regulatory proteins, and antioxidant properties remain insufficiently understood. In this study, fresh leaves (AS-FRE), dried leaves (AS-DRY), and stir-fried leaves (AS-STF) were comparatively analyzed using integrated metabolomics and proteomics, together with antioxidant activity evaluation in H_2O_2-induced HepG2 cells. The results showed that stir-frying markedly altered the chemical composition of *Aquilaria sinensis* leaves, especially by promoting the accumulation of flavonoids, terpenoids, and other secondary metabolites. Proteomic analysis further indicated that stir-frying enhanced the expression of proteins associated with secondary metabolite biosynthesis and related metabolic pathways. In addition, AS-STF exhibited stronger protective effects against oxidative stress than AS-DRY and AS-FRE, as evidenced by reduced lipid peroxidation and enhanced antioxidant enzyme activities. Overall, these findings suggest that stir-frying is an effective processing method for improving the functional value of *Aquilaria sinensis* leaves and provide a theoretical basis for the development of plant-derived antioxidants, functional teas, and related health products.

1. Introduction

Aquilaria sinensis leaf is a natural herbal beverage derived from the leaves of the *Aquilaria sinensis* tree. It is highly regarded for its distinctive aroma and a wide range of health-promoting properties, making it a significant component of traditional cultures, particularly in Southeast Asia. Historically, *Aquilaria sinensis* leaf has been utilized not only as a daily health tonic but also for its therapeutic effects in the treatment of gastrointestinal discomfort, the alleviation of inflammation, and the sedation of the nervous system, among other medicinal purposes (S. Wang et al., 2024). In recent years, *Aquilaria sinensis* leaf has attracted significant attention from the scientific community due to its rich bioactive chemical constituents.

With the continuous advancement in the study of plant functional substances, significant progress has been made in food processing, secondary metabolite regulation, and antioxidant mechanisms. Numerous studies have shown that the regulation of plant secondary metabolites plays an important role in food processing, particularly through methods such as thermal processing, enzymatic hydrolysis, and fermentation, which have been widely applied to enhance the bioavailability and stability of plant functional components. For example, enzymatic hydrolysis can specifically control enzymes within plant tissues to optimize the release and stability of bioactive components, thereby improving the functionality of plant-based products (Fonseca et al., 2025; Mu et al., 2024). In addition, fermentation not only improves the bioactivity of plant constituents but also promotes the synthesis of key secondary metabolites (such as flavonoids and polyphenols) through the action of microorganisms. The application of these

* Corresponding author.
E-mail address: yyliu@implad.ac.cn (Y. Liu).

https://doi.org/10.1016/j.fochx.2026.103808
Received 30 September 2025; Received in revised form 16 March 2026; Accepted 31 March 2026
Available online 1 April 2026

methods not only facilitates the extraction of functional substances but also enhances the antioxidant, antimicrobial, and anti-inflammatory health effects of foods by regulating metabolic pathways (Niyigaba et al., 2025).

These technologies offer advantages in reducing energy cons umption and maintaining the stability of plant bioactive components, particularly by minimizing thermal degradation while improving metabolite extraction efficiency. For instance, microwave heating selectively targets plant cells, thereby more effectively releasing intrinsic antioxidant compounds and significantly enhancing antioxidant activity (Joardder & Karim, 2025).

Among the various secondary metabolites present in *Aquilaria sinensis* leaves, we focused on flavonoids, terpenoids, and phenolic acids due to their known antioxidant properties and potential health benefits. These compounds were selected based on their abundance in the leaves and their relevance to the biological activity associated with oxidative stress protection. However, in contrast to the extensive research on *Aquilaria sinensis* wood, studies on the chemical composition and functional properties of *Aquilaria sinensis* leaves remain relatively limited. Previous studies have extensively investigated the chemical composition and antioxidant properties of *Aquilaria sinensis* (Liu et al., 2021). However, these studies primarily focus on the wood, with limited research on the leaves, especially with regard to how different processing techniques influence bioactive compound profiles. This study aims to fill this gap by exploring the effects of stir-frying, drying, and fresh processing on the chemical and antioxidant properties of *Aquilaria sinensis* leaves, offering novel insights into the functional enhancement of this plant material.

Recent investigations have begun to explore how different processing methods affect the composition and bioactivity of *Aquilaria sinensis* leaves. Traditional preparation techniques such as natural air-drying, stir-frying, and fresh use have been shown to alter the concentration, stability, and bioavailability of key phytochemicals. For instance, thermal processing may enhance the release of certain flavonoids while reducing heat-sensitive compounds such as some polyphenols or volatile terpenoids (Ahmed et al., 2024). Conversely, minimal processing of fresh leaves preserves a broader spectrum of native metabolites but may also lead to enzymatic degradation during storage. Despite these preliminary findings, comparative studies specifically focusing on the differences in metabolite profiles and potential bioactivities among fresh, naturally dried, and stir-fired *Aquilaria sinensis* leaves remain scarce.

Recent advancements in scientific technologies, particularly proteomics and metabolomics, have become indispensable tools for investigating the bioactivity and mechanisms of action of *Aquilaria sinensis* leaf. Proteomics, by analyzing protein expression profiles in biological systems, helps identify key regulatory proteins involved in complex biological processes. This approach can reveal how bioactive components in food interact with signaling pathways or influence physiological processes, providing insight into the molecular mechanisms behind their health benefits. Similarly, metabolomics focuses on analyzing small molecule metabolites and their metabolic pathways. By applying metabolomics to *Aquilaria sinensis* leaf, we can systematically explore its chemical composition, metabolite distribution, and the roles these metabolites play in metabolic pathways, offering comprehensive evidence to understand its bioactivity. This integrated approach allows for the quantitative analysis and functional prediction of the health effects of key metabolites in *Aquilaria sinensis* leaf.

Importantly, the integration of proteomics and metabolomics offers a complementary and more holistic perspective on the bioactivity of *Aquilaria sinensis* leaf. While metabolomics provides insight into the end products of cellular processes and reflects the actual biochemical status under specific conditions, proteomics helps identify the upstream regulatory proteins and pathways responsible for these metabolic changes. By combining these two approaches, researchers can establish correlations between metabolic outcomes and their regulatory networks, enabling a more precise elucidation of the mechanisms by which processing affects the functional properties of the leaves (Guo & Jia, 2025). We hypothesize that this integrated strategy could enhance the reliability and depth of functional food studies, particularly when exploring complex plant systems with diverse bioactive components. Further research is needed to confirm these potential benefits.

To achieve our research objectives, we designed experiments to compare the chemical composition and antioxidant activity of fresh, dried, and stir-fried *Aquilaria sinensis* leaves. This comparative analysis allows us to assess how different processing methods influence the bioactivity of the leaves, providing insights into their potential applications in functional foods and health products. Therefore, the focus of this research will be on the metabolite profiles and protein regulatory networks altered during processing, as well as how these molecular-level changes translate into phenotypic differences. An in-depth exploration of these issues will help elucidate the scientific connotations of traditional processing techniques and provide a solid theoretical foundation for the development of modern functional tea products.

2. Materials and methods

2.1. Experimental instruments

Mass spectrometer (TripleTOF 6600+, SCIEX), ultra-high-performance liquid chromatograph (LC-30 A, Shimadzu), ultra-high-performance liquid chromatograph (LC-30 A, Shimadzu), centrifuge (5424R, Eppendorf), constant temperature metal shaker (MU-G02–0448, Hangzhou MIO Instrument Co., Ltd.), analytical balance with a resolution of 0.0001 g (MS105DM, Mettler Toledo Instruments Co., Ltd.), centrifugal concentrator (CentriVap, LABCONCO), vortex mixer (VORTEX-5, Kyllin-Bell), ultrasonic cleaner (KQ5200E, Kunshan Instrument Co., Ltd.), Mouse Macrophages RAW 264.7 (Shanghai Institutes for Life Sciences, Chinese Academy of Sciences).

2.2. Experimental materials

Methanol (HPLC grade, Merck, Cat. No.: 1.06007.4008), acetonitrile (HPLC grade, Merck, Cat. No.: 1.00030.4008), formic acid (HPLC grade, Aladdin, Cat. No.: 695076-100ML), anhydrous ethanol (Xilong Chemical Co., China).

2.3. Collection and preparation of Aquilaria sinensis leaf samples

A total of 300 g of *Aquilaria sinensis* leaves from the same source were collected and processed by Guangdong Qinanxiang Biological Research Co., Ltd. The leaves were divided into three equal parts for different treatments. The first part (100 g) was used as the fresh sample, which was immediately frozen in liquid nitrogen after collection. The second part was naturally dried under sunlight. The third part of the sample underwent a series of processing steps, including withering, shaking, fermentation, and stir-frying. During the fermentation step, the samples were placed in a fermentation chamber at 30 °C for 48 h, with continuous stirring at 120 rpm to ensure uniform fermentation. Following fermentation, the samples proceeded to the stir-frying process, where the de-enzyming (kill-green) step was carried out in a traditional Chinese wok with a flat bottom. The temperature of the wok was monitored using a digital thermometer, maintaining a steady temperature of approximately 85 °C throughout the process. Each stir-frying session lasted 5 min and was repeated twice, resulting in a total heat treatment time of about 10 min. During the stir-frying process, the humidity was controlled at 60–65% using a humidity control system to ensure optimal enzymatic deactivation and metabolite retention. Subsequently, the samples were placed in a drying oven at 80 °C for 4 h to produce the stir-fried sample.

2.4. Determination of protein in Aquilaria sinensis leaf

2.4.1. Protein extraction

Frozen *Aquilaria sinensis* leaf samples were removed from −80 °C storage and briefly thawed on ice to maintain protein integrity. The samples were then ground into fine powders in liquid nitrogen. Appropriate amounts of powders were transferred to 1.5 ml centrifuge tubes, and sufficient volumes of L3 lysis buffer (1% SDS, 100 mM Tris-HCl, 7 M urea, 2 M thiourea, 1 mM PMSF, and 2 mM EDTA) were added. After mixing by shaking, the samples were sonicated on ice for 10 mins, and the supernatants were collected by centrifugation to obtain the protein solutions. Four times the volume of cold acetone was added to the protein solutions, and the mixtures were precipitated overnight at −20 °C. The precipitates were retained by centrifugation at 4 °C and washed three times with cold acetone. The precipitates were then re-dissolved in 8 M urea, and the total protein concentrations were determined using BCA protein assay kits (Shanghai Biyuntian Biotechnology Co., Ltd.)(Feng et al., 2012).

2.4.2. Protein digestion

Take 100 μg of the protein solution from Section 2.4.1 and adjust the volume to 200 μL using 8 M urea. Add DTT to a final concentration of 5 mM and incubate at 37 °C for 45 min for reduction. Then, alkylate the sample in the dark at room temperature with iodoacetamide (final concentration 11 mM) for 15 min. Next, add 800 μL of 25 mM ammonium bicarbonate solution and 2 μL of trypsin (Promega, V5280), and digest overnight at 37 °C. After digestion, adjust the pH to approximately 2–3 using 20% TFA, and desalinate the peptide mixture using a C18 column (Millipore, Billerica, MA). Finally, determine the peptide concentration using the Pierce™ Quantitative Colorimetric Peptide Assay Kit (Thermo Fisher) according to the manufacturer's instructions.

2.4.3. Data-independent acquisition (DIA) LC-MS/MS analysis

Peptide samples were reconstituted and analyzed on an Easy-nLC 1200 coupled to a Q Exactive HF-X Orbitrap mass spectrometer (Thermo Fisher Scientific, USA) operated in data-independent acquisition (DIA) mode. Peptides were loaded onto a C18 reversed-phase column and separated with a linear acetonitrile gradient (0.1% formic acid) over 16 min. The mass spectrometer acquired MS1 survey scans at 60,000 resolution (at *m/z* 200) over m/z 390 to 1010 (AGC target 1e6, maximum injection time 60 ms), followed by sequential MS/MS scans using 75 contiguous isolation windows of approximately 8 m/z spanning m/z 400 to 1000. MS2 scans were collected at 15,000 resolution (AGC target 1e6, injection time 20 ms) with higher-energy collisional dissociation (HCD) at normalized collision energy (NCE) 27.

2.4.4. Data processing and protein identification

DIA raw files were processed with DIA-NN v.1.8 (Demichev et al., 2020) in library-free mode against a custom protein database derived from our transcriptome using open reading frames predicted by TransDecoder (Haas et al., 2013). Peptide and protein-level false discovery rates were controlled at 1% using a target-decoy strategy. Protein quantification was based on interference-corrected fragment ion intensities with run-wise normalization. Identified proteins were matched to their corresponding unigenes and annotated with KEGG Orthology (KO) identifiers.

2.5. Metabolite collection and identification of Aquilaria sinensis leaf

2.5.1. Preparation of test samples

For each type of *Aquilaria sinensis* leaf, 2.0 g of the sample was weighed and mixed with 50.00 mL of distilled water. The mixture was maintained at a boiling state under a water bath condition with continuous condensation and reflux for 2 h. After cooling, the solution was filtered and transferred into a pre-dried evaporation dish that had been dried to a constant weight. The filtrate was evaporated to dryness on a water bath and further dried at 105 °C for 3 h. The dried residue was then cooled in a desiccator for 30 mins and accurately weighed. The dried extract was reconstituted with an appropriate solvent to a final concentration of 1 mg/mL. Terpenoid compounds were identified using Liquid Chromatography–Mass Spectrometry (LC-MS) as described in Section 2.5.2.

Next, 100 μL of the reconstituted solution was transferred into a 1.5 mL centrifuge tube, vortexed for 15 mins, and centrifuged at 12,000 r/min at 4 °C for 3 mins. The supernatant was collected, filtered through a 0.22 μm microporous membrane, and stored in an autosampler vial for subsequent LC-MS/MS analysis.

2.5.2. Chromatography-mass spectrometry collection conditions

Use a Waters ACQUITY UPLC HSS T3 column (1.8 μm, 2.1 mm × 100 mm) with 0.1% formic acid in water as mobile phase A and 0.1% formic acid in acetonitrile as mobile phase B. Set the column temperature to 40 °C, with a flow rate of 0.4 mL/min, and inject a sample volume of 4 μL. Perform gradient elution according to the mass spectrometry conditions in Table 1 and the following mobile phase program: start with 95% of mobile phase A. At the 5th minute, reduce mobile phase A to 35%, then decrease to 1% at 6 mins and hold for 1.5 mins. At 7.6 mins, return to 95% and maintain this condition until the end of the run at 10 mins (Jiang, Hou, et al., 2024).

2.6. Antioxidant activity assay

2.6.1. Cell culture

HepG2 cells were retrieved from liquid nitrogen storage and rapidly thawed in a 37 °C water bath. The thawed cell suspension was immediately transferred into a 15 mL centrifuge tube, and 2 mL of complete culture medium was added to resuspend the cells, ensuring thorough mixing with the medium. The suspension was centrifuged at 1000 rpm for 5 mins, after which the supernatant was carefully discarded. The cell pellet was then resuspended in an appropriate volume of complete culture medium and transferred to a culture flask containing medium supplemented with 10% fetal bovine serum (FBS). The flask was placed in a 37 °C incubator with 5% CO2 for cell culture. When the cells reached approximately 90% confluency, 1 mL of trypsin was added to the culture vessel for enzymatic digestion. Once detachment was complete, an equal volume of complete culture medium was immediately added to neutralize the trypsin. The cell suspension was then transferred into a centrifuge tube and centrifuged at 1000 rpm for 5 mins. The supernatant was discarded, and the cell pellet was resuspended in 3 mL of complete culture medium, followed by gentle pipetting to ensure even cell dispersion. The resuspended cells were evenly distributed into 10 cm culture dishes, gently swirled to ensure uniform distribution, and then placed back into the incubator for continued culture under standard conditions (Xiaowen et al., 2021).

Table 1
Chromatographic and mass spectrometric acquisition conditions.

Parameter name	ESI+	ESI-	Parameter name	ESI+	ESI-
Duration (min)	10	10	Declustering Potential (V)	60	−60
IonSpray Voltage (V)	5000	−4000	MS1 Collision Energy (V)	10	−10
Temperature (°C)	550	550	MS2 Collision Energy (V)	30	−30
Ion Source Gas 1 (psi)	50	50	Collision Energy Spread (V)	15	15
Ion Source Gas 2 (psi)	60	60	MS1 TOF Massess (Da)	50–1250	50–1250
Curtain Gas (psi)	35	35	MS2 TOF Massess (Da)	25–1250	25–1250

2.6.2. Toxic effects of Aquilaria leaf on HepG2 cells

HepG2 cell culture and passage were performed according to the method described by Tang (Tang, 2020). Cells were seeded into 96-well plates at a density of 1×10^5 cells/mL, with 100 μL of cell suspension per well. The plates were incubated at 37 °C with 5% CO_2 for 24 h to allow cell attachment. After incubation, the spent culture medium was carefully removed. For the experimental treatment, the control group received serum-free DMEM medium, while the treatment groups were supplemented with different fractions of Aquilaria leaf extract at final concentrations of 3.125, 6.25, 12.50, 25.00, 50.00, 100.00, 200.00, 400.00, 800.00, and 1600.00 μg/mL. The cells were then incubated for an additional 24 h, with each concentration set up in six replicates per group. Following treatment, the old culture medium was removed, and 200 μL of MTT solution (final concentration: 0.50 mg/mL) was added to each well. The plates were then incubated in a CO_2 incubator for 4 h. After incubation, the supernatant was carefully discarded, and 150 μL of DMSO was added to each well. The plate was protected from light and shaken for 10 mins to fully dissolve the formazan crystals. The optical density (OD) was measured at 490 nm, and the cell viability was calculated accordingly.

$$\text{Cell viability (\%)} = OD_{experiment}/OD_{control} \times 100\%$$

2.6.3. Measurement of indicators related to antioxidant enzyme activity

SOD activity was measured using a WST-1 assay kit (Sigma-Aldrich), with the reaction system consisting of 5 mM horseradish peroxidase, 3 mM superoxide, and buffer solution; each reaction was incubated for 10 min, and absorbance was recorded at 450 nm. CAT activity was determined using a CAT activity assay kit, with reactions performed in 20 mM H_2O_2 and pH 7.4 buffer solution, and absorbance measured at 240 nm after the reaction. GSH-PX activity was assayed using a kit from Cayman Chemical (USA), with absorbance measured at 340 nm. All measurements were conducted using a BioTek Synergy H1 multifunctional microplate reader, while CAT measurements were additionally performed with a PerkinElmer Lambda 25 spectrophotometer. HepG2 cells were seeded into 6-well plates at a density of 5 × 105 cells/mL and incubated at 37 °C with 5% CO_2 for 24 h. Oxidative stress was induced by treating the cells with 200 μmol/L H_2O_2, while different concentrations of stir-fried, fresh, and dried *Aquilaria sinensis* leaf extracts were simultaneously administered for 6 h. After treatment, the cells were collected, and SOD, MDA, CAT, and GSH-Px levels were measured following the method described by Ji et al. (Ji et al., 2024).

2.7. Statistical analysis and visualization of omics data

To comprehensively reveal the differential features of the metabolomic and proteomic datasets, multiple statistical models and visualization methods were employed. First, Principal Component Analysis (PCA) was performed to reduce dimensionality and evaluate both inter-group differences and intra-group reproducibility. PCA was conducted in R software (v4.2.0), and the results were visualized as two-dimensional scatter plots showing sample distribution and clustering (Zhiqiang et al., 2023).

For differential feature screening, Volcano plots were used to simultaneously represent statistical significance and fold changes. The volcano plot was generated using the R package ggplot2, and differential features were determined using $p < 0.05$ and $|\log2(FC)| > 1$. In addition, False Discovery Rate (FDR) correction was applied to the data using the Benjamini-Hochberg method to minimize the risk of type I errors due to multiple testing (Suguru et al., 2022).

To explore the co-regulation among differential metabolites/proteins, Pearson correlation coefficients were calculated and visualized as correlation heatmaps. The correlation matrix was plotted in R (v4.2.0), with color gradients representing the strength of correlations and clustering trees highlighting the similarity relationships among metabolites or proteins (Jeon et al., 2020). To control for false-positive associations arising from multiple comparisons in large-scale multi-omics data, the *p*-values obtained from the correlation analysis were further adjusted using the Benjamini-Hochberg false discovery rate (FDR) method. Only correlations meeting the predefined coefficient threshold and FDR-adjusted significance level were retained for downstream interpretation.

Additionally, hierarchical clustering heatmaps were generated to intuitively display the expression patterns of differential metabolites and proteins. Both samples and variables were clustered based on Euclidean distance and complete linkage. Heatmaps were visualized in R (v4.2.0) using the ComplexHeatmap package (v2.12.0), with color gradients indicating relative abundance levels (Jeon et al., 2020).

3. Results

3.1. The metabolomics and component changes in Aquilaria sinensis leaf

The overall metabolite composition of fresh, dried, and stir-fried *Aquilaria sinensis* leaves exhibits notable variations. To comprehensively understand the impact of the stir-frying process on metabolic changes in *Aquilaria sinensis* leaves, we conducted metabolomic and proteomic analyses on these three sample types.

Metabolomic and proteomic analyses were performed on three *Aquilaria sinensis* leaf samples: fresh (AS-FRE), naturally dried (AS-DRY), and stir-fried (AS-STF), to comprehensively investigate the effects of processing methods on their metabolic profiles.

As illustrated in Fig. 1(A), although the overall distribution of major metabolite classes was comparable among the samples, quantitative differences were observed. Flavonoids represented the predominant metabolite category in all samples, accounting for approximately 20% (relative percentage content; the other data presented in this section also represent relative percentage content) of the total metabolites. The flavonoid proportions were 20.71% in AS-STF, 20.38% in AS-FRE, and 20.20% in AS-DRY. Amino acids and their derivatives, together with alkaloids, accounted for 13.41% in both AS-FRE and AS-STF, while AS-DRY showed a proportion of 13.65%.

For lipids and phenolic acids, the relative proportions were also comparable among the three samples. Lipids accounted for 9.14% in AS-STF, 9.11% in AS-FRE, and 9.10% in AS-DRY. Phenolic acids represented 8.19% in AS-FRE, 8.16% in AS-STF, and 8.02% in AS-DRY. Terpenoid compounds accounted for 7.22% in AS-STF, 7.14% in AS-FRE, and 7.07% in AS-DRY. Lignans and coumarins accounted for 5.08% in AS-FRE, 5.00% in AS-STF, and 4.94% in AS-DRY. Minor metabolite classes, including organic acids, nucleotides and their derivatives, quinones, and tannins, were present at relatively low proportions across the samples.

The Venn diagram analysis (Fig. 1(B)) revealed substantial overlap and certain unique metabolites among the three sample types. A total of 2178 metabolites were commonly shared among AS-FRE, AS-DRY, and AS-STF, indicating high similarity in their chemical profiles. Additionally, AS-STF shared 44 metabolites individually with AS-FRE and AS-DRY. The Venn diagram showed that 41 unique metabolites were identified in AS-STF, indicating that stir-frying induced significant changes in the metabolic profile. These unique metabolites were primarily classified into three chemical classes: flavonoids, terpenoids, and phenolic acids. Flavonoids such as luteolin and quercetin are known for their antioxidant properties, while terpenoids like β-caryophyllene are involved in anti-inflammatory pathways. Phenolic acids, such as caffeic acid, have been linked to various health benefits, including antimicrobial activity. The identification of these metabolites, coupled with their bioactivity, underscores the significant metabolic impact of stir-frying on *Aquilaria sinensis* leaves.

The CV curve in Fig. 1(C) shows a high degree of overlap, indicating that while the differences between the treatments may appear subtle,

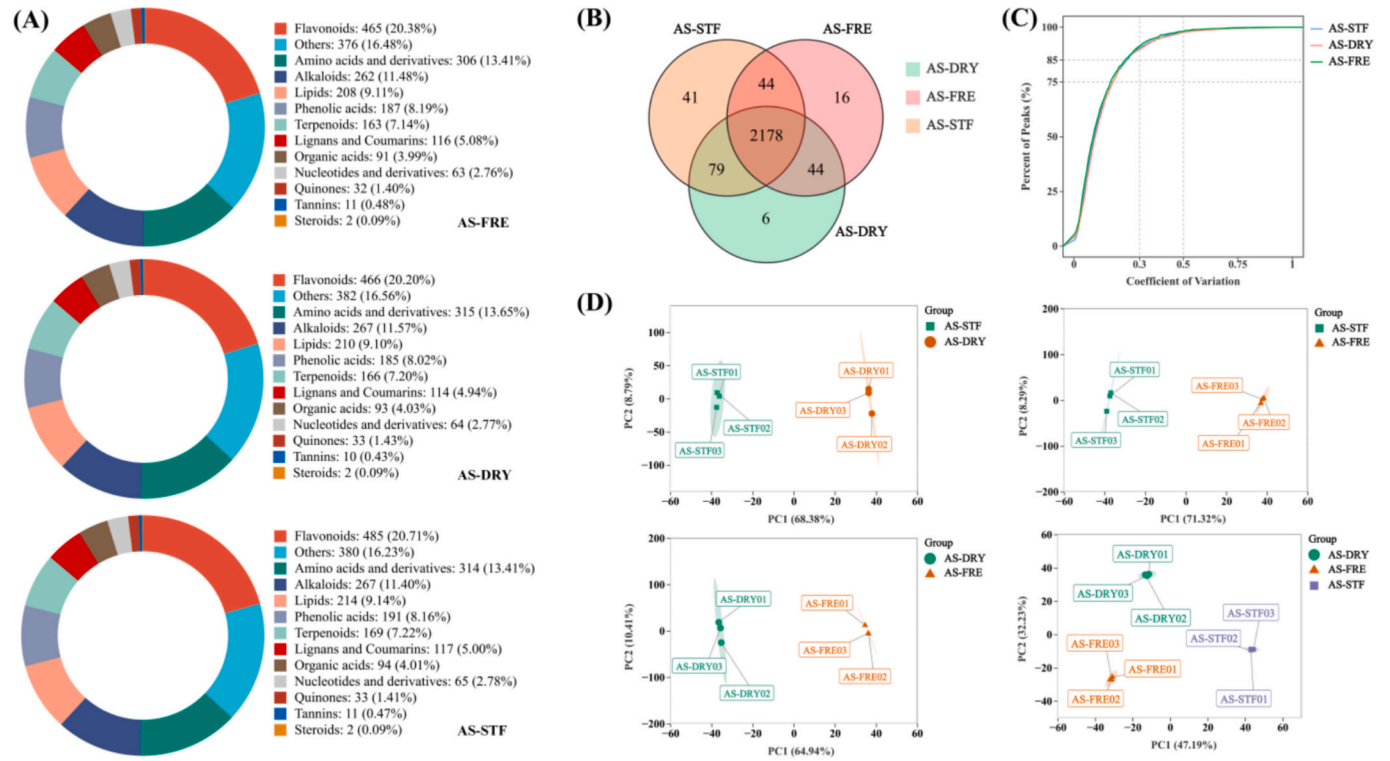

Fig. 1. Metabolomics and component changes in *Aquilaria sinensis* leaf (A: Metabolite composition of different *Aquilaria sinensis* leafs ; B:Venn diagram of components in different *Aquilaria sinensis* leafs ; C:Coefficient of variation (CV) distribution of components in different *Aquilaria sinensis* leafs ; D:Principal component analysis (PCA) plot of metabolomics data from different *Aquilaria sinensis* leafs (95% confidence intervals)).

this does not preclude significant metabolic differences. Specifically, PCA (Principal Component Analysis) revealed a clear separation between the stir-fried sample (AS-STF) and both the dried (AS-DRY) and fresh (AS-FRE) samples. This suggests that stir-frying induced distinct metabolic alterations despite the apparent overlap in the CV curve. The overlap observed in the CV curve primarily reflects general trends in metabolic variation, whereas PCA captures the global metabolic shifts, which may not be immediately visible through simpler methods like the CV curve.

Principal component analysis (PCA) (Fig. 1(D)) further elucidated compositional differences among samples under distinct processing conditions. On PC1 (68.38%), AS-STF samples clearly separated from AS-DRY, indicating significant differences in their metabolic profiles, with AS-DRY showing tighter clustering and AS-STF more dispersed. On PC2 (32.79%), partial overlap suggested similar metabolite compositions between AS-STF and AS-DRY. In the PCA comparison of AS-STF and AS-FRE along PC1 (71.32%), AS-STF exhibited more clustering, whereas AS-FRE displayed higher variability, suggesting notable differences induced by stir-frying. Comparing AS-DRY and AS-FRE, AS-DRY samples were more clustered on PC1 (64.94%) and PC2 (10.41%), reflecting lower metabolic variability relative to fresh samples. The overall PCA plot highlighted clear distinctions among AS-STF, AS-DRY, and AS-FRE, with AS-STF samples distinctly separated from the other two groups, emphasizing the significant metabolic impact of stir-frying. Notably, AS-DRY and AS-FRE also displayed considerable differences in their metabolic distributions.

The stir-frying process induced significant alterations in the chemical composition of *Aquilaria sinensis*, particularly increasing the concentrations of flavonoids and terpenoids. These results suggest that heat-induced modifications during stir-frying may facilitate the release or synthesis of certain bioactive compounds, as observed in the higher concentrations of flavonoids and terpenoids in the AS-STF compared to both the AS-DRY and the AS-FRE. This finding aligns with previous studies, which have shown that thermal treatments can enhance the bioavailability and stability of secondary metabolites in plant materials. However, further research is necessary to elucidate the specific mechanisms driving these changes, particularly regarding the influence of temperature and processing time on the metabolic pathways involved.

3.2. *Differential metabolite analysis in Aquilaria sinensis leaf*

The volcano plots (Fig. 2(A)) illustrate the differential metabolite profiles among the three sample groups: AS-STF, AS-DRY, and AS-FRE. In the AS-STF vs. AS-DRY comparison, 797 metabolites were significantly upregulated (purple), 581 were downregulated (blue), and 1014 exhibited no significant differences (gray). Similarly, in the AS-STF vs. AS-FRE comparison, 728 metabolites were upregulated, 726 were downregulated, and 948 showed no significant variation. A comparable trend was observed in another AS-STF vs. AS-FRE comparison, with 534 metabolites upregulated, 727 downregulated, and 1106 remaining unchanged.

The hierarchical clustering heatmap (Fig. 2(B)) visualizes the differential expression patterns of metabolites across the three sample groups, categorizing them into terpenoids, alkaloids, flavonoids, phenolic acids, amino acids and their derivatives, and other metabolic classes. Each row represents a metabolite, while columns correspond to the different sample groups. In the AS-STF vs. AS-DRY comparison, among the top 20 significantly different metabolites, 16 (including MWSSlk217, Cmqp003383, MWSHY0098, Yamp002097, Zaln004082, MWSslk042) were upregulated in stir-fried samples, whereas four (mws0055, Zahp00242, MWS0205, and Lmgn013947) exhibited higher expression in dried samples. Notably, MWSHY0098 and MWSHY0174 were identified as flavonoids. In the AS-STF vs. AS-FRE comparison, 18 metabolites, including Yamp002097, MWO155444, Wayp001024, pmb0864, and Zbsp004714, displayed elevated expression in stir-fried samples, whereas Lmjn004873 and Lmgn013947 were more abundant in fresh samples. Among the 20 significantly different metabolites in this comparison, Zbsp004714, Zbsp008132, Lmtp004044, Lazp005201, and

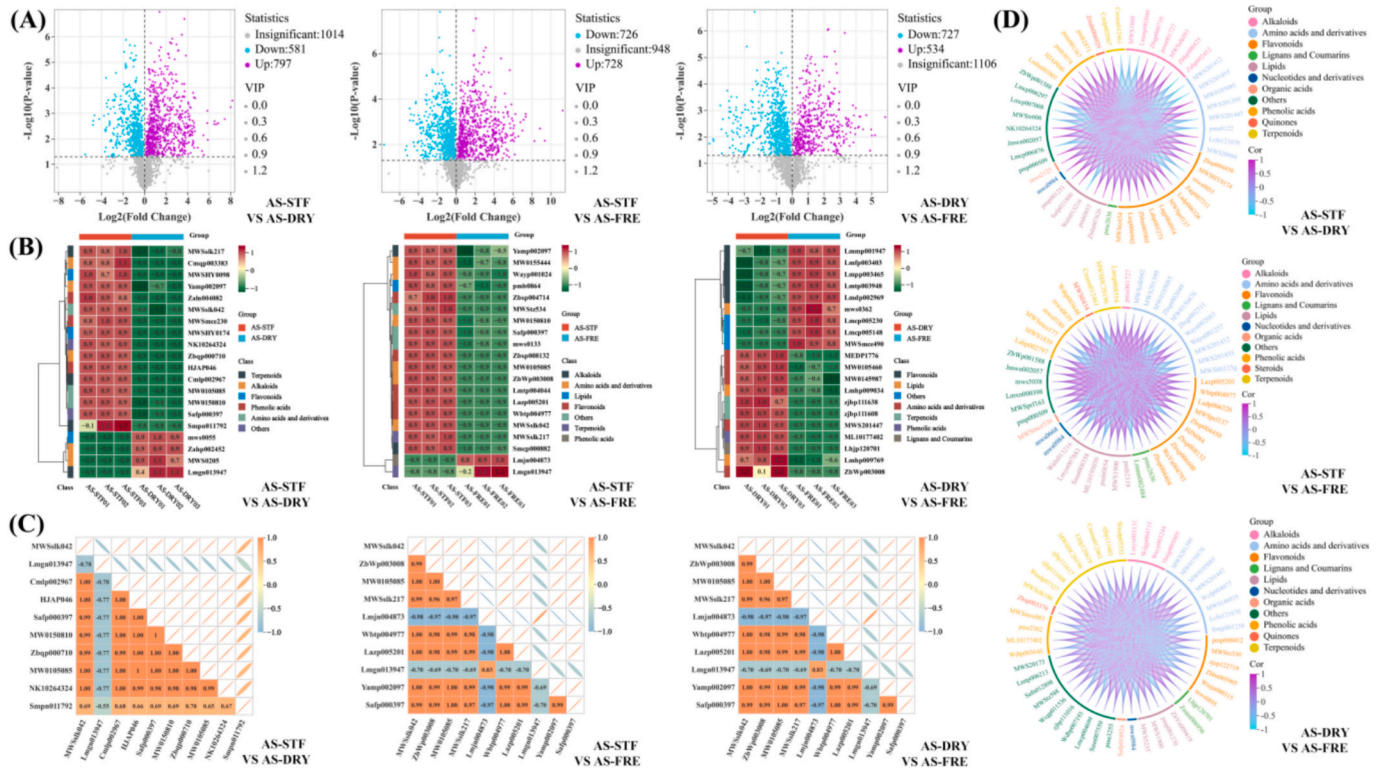

Fig. 2. Metabolite differences in *Aquilaria sinensis* leaf (A: Volcano plot of metabolite comparisons among different *Aquilaria sinensis* leafs (Fold Change >1.5, $p < 0.05$); B: Clustering heatmap of differential metabolites in different *Aquilaria sinensis* leaf samples; C: Correlation heatmap of differential metabolites in different *Aquilaria sinensis* leaf samples; D: Chord diagram of metabolite correlations in different *Aquilaria sinensis* leafs).

Wbtp004977 were identified as flavonoids.

To further elucidate the metabolic correlations among the different sample groups, a correlation heatmap was generated (Fig. 2(C)). In the AS-STF vs. AS-DRY comparison, MWSSlk042 exhibited a strong positive correlation (0.99) with Safp000397, indicating a consistent expression trend in stir-fried and dried samples, whereas Lmgn013947 showed a negative correlation (−0.78) with Safp000397, suggesting an opposing expression pattern. Additionally, Cmlp002967 and MWO150585 demonstrated a negative correlation (−0.77), reflecting distinct metabolic responses in these processing conditions. HjAP046 displayed high positive correlations with multiple metabolites, particularly with MWO150585 (0.9), indicating a strong association between their expression patterns. Similarly, MWO150585 and Zbqp000710 exhibited a strong positive correlation (0.99), suggesting their synchronized expression changes. Conversely, NK10264324 and Cmlp002967 demonstrated a negative correlation (−0.77), further highlighting their differential responses between stir-fried and dried samples.

In the AS-DRY vs. AS-FRE comparison, MWSSlk042 exhibited strong positive correlations with both ZbWp003008 (0.99) and MWO150585 (0.99), indicating similar expression patterns in dried and fresh samples. Additionally, MWSSlk217 showed a strong correlation with MWO150585 (0.99) and ZbWp003008 (0.99), further reinforcing the consistency in metabolic regulation. In contrast, Lmjn004873 and MWO150585 displayed a strong negative correlation (−0.97), reflecting divergent metabolic responses in dried and fresh samples. The positive correlation between Wbtp004977 and Lazp005201 (0.98) suggests a parallel expression pattern, whereas the strong correlation between Lazp005201 and MWSSlk042 (0.99) indicates co-regulation in dried and fresh samples. Conversely, Lmgn013947 and ZbWp003008 showed a negative correlation (−0.70), supporting their distinct metabolic expression in these two sample groups.

In the AS-STF vs. AS-FRE comparison, MWSSlk042 exhibited a strong positive correlation with MWO150585 (1.0) and ZbWp003008 (1.0), signifying highly synchronized metabolic variations between stir-fried and fresh samples. Similarly, MWSSlk217 showed a strong correlation (0.99) with MWO150585 and ZbWp003008, reinforcing the consistent metabolic responses in these processing conditions. However, Lmjn004873 and MWO150585 exhibited a strong negative correlation (−0.97), indicating opposing expression patterns. The positive correlation between Wbtp004977 and Lazp005201 (0.98) suggests a similar metabolic trend, while the strong correlation between Lazp005201 and MWSSlk042 (1.0) highlights their tightly linked metabolic expression. Conversely, Lmgn013947 and ZbWp003008 demonstrated a negative correlation (−0.69), suggesting significant metabolic differentiation between stir-fried and fresh samples.

Furthermore, a differential correlation chord diagram was employed to visualize the metabolite correlations across the three sample groups. In the AS-STF vs. AS-DRY comparison, metabolites such as MWSSlk042, MWSSlk217, MWO150585, MWSSlk042, and Lmgn013947 exhibited high correlation values (close to 1), indicating similar metabolic behavior. In contrast, the negative correlation between Safp000397 and Zbqp000710 suggests opposing metabolic trends in these two groups. In the AS-STF vs. AS-FRE comparison, metabolites including MWO150585, ZbWp003008, MWSSlk042, and Safp000397 exhibited strong correlations, suggesting a high degree of metabolic synchronization between stir-fried and fresh samples. However, Lmgn013947 exhibited a strong negative correlation in fresh samples compared to stir-fried samples, indicating that the stir-frying process might downregulate its expression. Lastly, in the AS-DRY vs. AS-FRE comparison, MWSSlk042, MWSSlk217, and MWO150585 displayed high positive correlations, demonstrating that these metabolites follow similar expression patterns between dried and fresh samples.

3.3. Proteomics and differential expression analysis in Aquilaria sinensis leaf

Principal component analysis (PCA) was conducted to evaluate the proteomic variations among AS-STF, AS-DRY, and AS-FRE sample groups. As illustrated in Fig. 3(A), PC1 (48.14%) and PC2 (16.18%) captured the major variance in protein composition across different processing conditions. A clear separation between AS-STF and the other two groups (AS-DRY and AS-FRE) underscored the substantial impact of stir-frying on the proteome, distinguishing it significantly from drying and fresh samples. AS-FRE samples exhibited a more dispersed distribution, indicating a higher degree of proteomic diversity, while AS-DRY samples were more tightly clustered, reflecting the uniform influence of the drying process on protein composition.

Fig. 3**(B)** presented the correlation analysis of protein expression across AS-STF, AS-DRY, and AS-FRE. A high positive correlation was observed between AS-STF and both AS-DRY and AS-FRE, with correlation coefficients close to 0.9 for AS-STF01 vs. AS-DRY01 and AS-FRE01. This suggested a degree of similarity between the stir-fried samples and the other two groups, albeit with notable differences in specific protein expressions. The within-group correlation among AS-DRY samples was exceptionally high (close to 1.0), indicating strong consistency in proteomic composition following drying. Similarly, AS-FRE samples also exhibited strong correlations ($\geq$0.96), demonstrating a high degree of similarity in protein expression patterns within the fresh sample group. Despite the overall high correlations between AS-STF and the other two groups, distinct proteomic differences were evident, particularly in the expression of certain proteins.

Differentially expressed protein (DEP) analysis using volcano plots **(**Fig. 3(C)**)** further highlighted the impact of processing on the proteome. In the AS-STF vs. AS-DRY comparison, 26 proteins were significantly downregulated, 15 were upregulated, and 104 exhibited no significant change. While the majority of proteins showed minor expression variations, a subset displayed pronounced alterations. In the AS-STF vs. AS-FRE comparison, 35 proteins were downregulated, 17 were upregulated, and 94 showed no significant difference, suggesting that stir-frying induced substantial proteomic changes compared to fresh samples, particularly with a greater number of downregulated proteins. Similarly, in the AS-DRY vs. AS-FRE comparison, the number of differentially expressed proteins mirrored that of the AS-STF vs. AS-FRE comparison, with 35 proteins downregulated, 17 upregulated, and 94 unchanged.

Fig. 3 **(D)** quantitatively assessed the number of differentially expressed proteins across the three groups, categorizing them as upregulated, downregulated, and total DEPs. In the AS-DRY vs. AS-STF comparison, 18 proteins were upregulated, 2 were downregulated, with a total of 20 DEPs. In the AS-FRE vs. AS-STF comparison, 35 proteins were upregulated, 15 were downregulated, amounting to 50 DEPs. The AS-FRE vs. AS-DRY comparison exhibited the highest number of DEPs, with 52 upregulated, 26 downregulated, and a total of 78 differentially expressed proteins.

A heatmap **(**Fig. 3(E)**)** further visualized the relative expression levels of DEPs across the different sample groups. Several proteins, including AWK57838.1, AWK9261.1, AMQ67166.1, and ZNB54699.1, were markedly upregulated in AS-STF, suggesting that stir-frying enhanced their expression. Conversely, these proteins exhibited lower expression in AS-FRE, appearing green on the heatmap, indicating a downregulatory effect of the fresh state. Additionally, proteins such as AWN29367.1, QNX35558.1, and ACF73365.1 were more highly expressed in fresh samples but downregulated in stir-fried samples.

In the AS-STF vs. AS-DRY comparison, ATJJ0061.1 displayed significantly higher expression in AS-STF, as indicated by deep red coloration, whereas its expression was lower in AS-DRY. Similarly, UNJ25381.1 exhibited markedly higher expression in AS-STF compared to AS-DRY, indicating that stir-frying promoted its expression. In

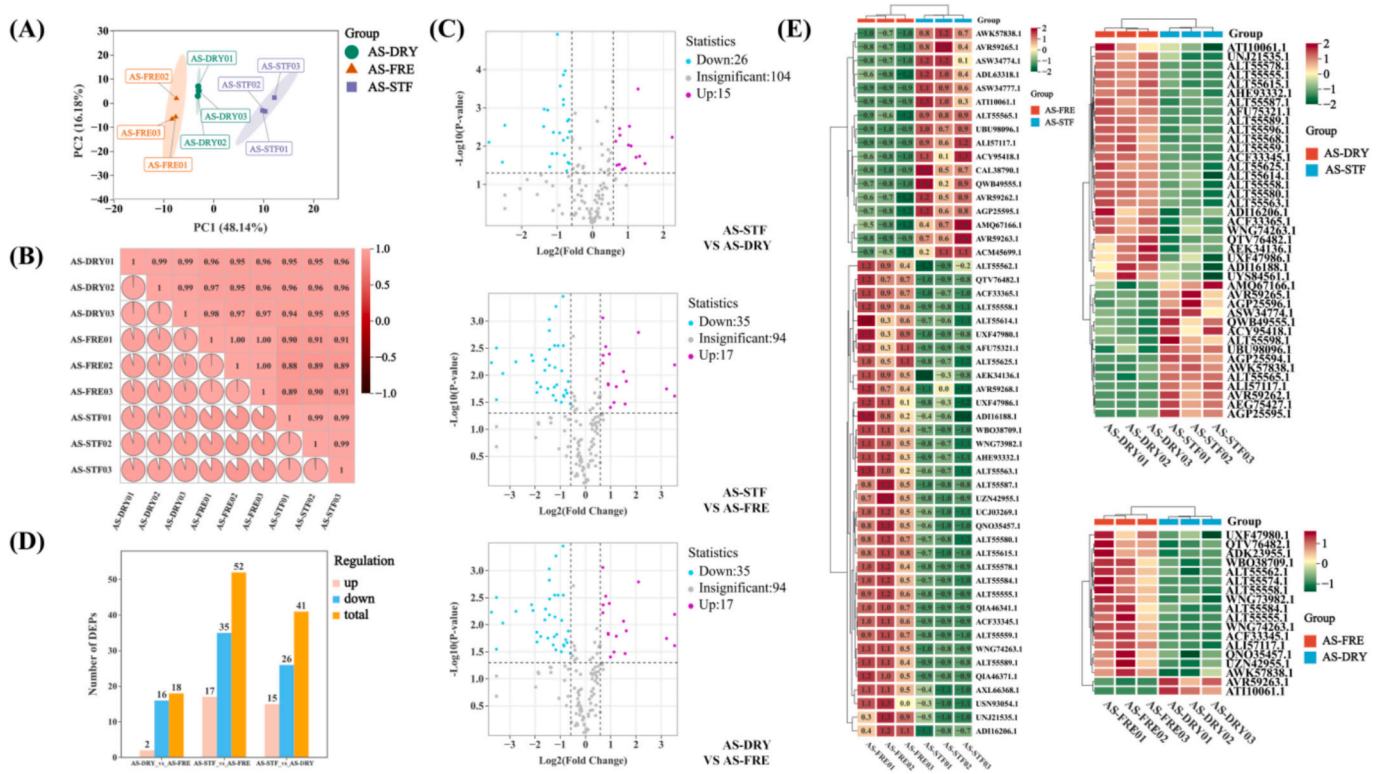

Fig. 3. Proteomics and differential expression analysis in *Aquilaria sinensis* leaf (A: Principal component analysis (PCA) plot of proteomics data from different *Aquilaria sinensis* leafs (95% confidence intervals); B: Correlation analysis of differentially expressed proteins in different *Aquilaria sinensis* leafs; C:Volcano plot analysis of differentially expressed proteins in different *Aquilaria sinensis* leafs (Fold Change >1.5, $p < 0.05$); D: Statistical analysis of the number of differentially expressed proteins in different *Aquilaria sinensis* leafs; E: Clustering heatmap of differentially expressed proteins in different *Aquilaria sinensis* leafs).

contrast, proteins such as AL155528.1 and AWT25308.1 were more highly expressed in AS-DRY, appearing in red, whereas their expression was suppressed in AS-STF, appearing in green. This suggested that the drying process upregulated their expression, whereas stir-frying may have exerted an inhibitory effect. In the AS-FRE vs. AS-DRY comparison, proteins UXF47980.1, QTV76482.1, and ADK23955.1 exhibited higher expression levels in AS-FRE. Conversely, proteins WBO38709.1, ALT55561.1, and ACF33345.1 were upregulated in AS-DRY samples, represented in red, highlighting the impact of drying on increasing their expression.

3.4. Joint analysis of metabolite and protein expression differences in *Aquilaria sinensis* leaf

In the *Aquilaria sinensis* leaf experiment, a total of 1210 differential metabolites and 61 differential proteins were identified. Among the differential metabolites, 126 were alkaloids, 159 were amino acids and derivatives, 206 were flavonoids, 48 were lignans and coumarins, 139 were lipids, 22 were nucleotides and derivatives, 46 were organic acids, 218 were classified as others, 125 were phenolic acids, 11 were quinones, 1 was a steroid, 5 were tannins, and 104 were terpenoids.

The top ten significantly different metabolites (Table 3) included Wmyn000214 (Gentisic acid 5-O-β-D-(6'-O-galloyl)-glucopyranoside), Lazn003893 (Erythro-Guaiacylglycerol-β-Coniferyl Ether), Qmyp101402 (11,12-O-Isopropyfidenesolajiangxin F), Wasdp07327 (β-Rotunol), Lmmn006932 (2-Hydroxy-4-methyl-3-tridecanoyloxypentanoic acid methyl ester), Hmqn003054 (9,10,11-Trihydroxy-12-octadecenoic acid), Lmtp005226 (Santalol), Wbsp010227 (3β,14α,15α,29α-tetrahydroxyserrat-14-en-3-(3′-methoxyl-4′-hydroxybenzoate)), zjbp111605 (9-Hydroxyselina-3,11-dien-12-al), and Wafn011571 (α-Hydroxylinoleic acid). The top ten significantly different flavonoids (Table 3) included Zbgp007629 (3′,4'-Dihydroxy-7,5′-dimethoxyflavone), Lamn006359 (4′-demethyl-3,9-dihydroeucomin glucoside), Zbbn005905 (Abyssinone II), MWS20147 (Luteolin-3'-O-glucoside), Hmqn003268 (Dihydrotricetin), Cmsp006026 (Dihydrorhamnetin), pmp000596 (Quercetin-3-O-(2"-O-galactosyl)glucoside), Xmgp006913 (2,4,2′,4′-tetrahydroxy-3′-prenylchalcone), MWSHY0058 (Luteolin), and Wbtn006810 (6,7-dihydroxy-1,3-dimethoxyxanthen-9-one).

Fig. 4(A) illustrates the KEGG enrichment analysis of differential metabolites and proteins (Table 2). The enrichment results suggested that biosynthesis of secondary metabolites and flavonoid biosynthesis were among the major pathways associated with the differences between AS-STF and AS-DRY. Additionally, the biosynthesis of amino acids and flavonoid biosynthesis pathways also exhibited significant enrichment. In proteomic enrichment analysis, carbon metabolism and biosynthesis of secondary metabolites were highly enriched, indicating that regulation at the protein expression level plays a critical role in the physiological properties of *Aquilaria sinensis* leaves. Notably, the enrichment of glyoxylate and dicarboxylate metabolism, as well as plant hormone signal transduction pathways, suggests that these pathways may modulate *Aquilaria sinensis* leaf growth, development, and stress resistance. These findings provide pathway-level clues for understanding the coordinated changes in proteins and metabolites induced by stir-fried processing. However, the KEGG enrichment results in this study are based on omics-level association analysis and mainly serve as supportive evidence for potential biological interpretation, rather than direct experimental validation of specific pathway regulation.

From the perspective of "protein–pathway–metabolite" co-occurrence, AGP25594.1 (K00487) and AGP25596.1 (K01859, CHI) both point to the core flavonoid biosynthesis pathway, suggesting their role as potential "bottleneck sites" driving flavonoid skeleton formation under AS-STF conditions. CHI, as the early key enzyme catalyzing the conversion of chalcone to flavanone, is often regarded as one of the flux control points. Meanwhile, ADK23955.1 (K02183), corresponding to calmodulin, is consistent with the enrichment of MAPK and plant hormone signaling transduction (ko04016/ko04075), indicating that Ca^{2+} may function as a cross-pathway "signal hub" in the regulation of the

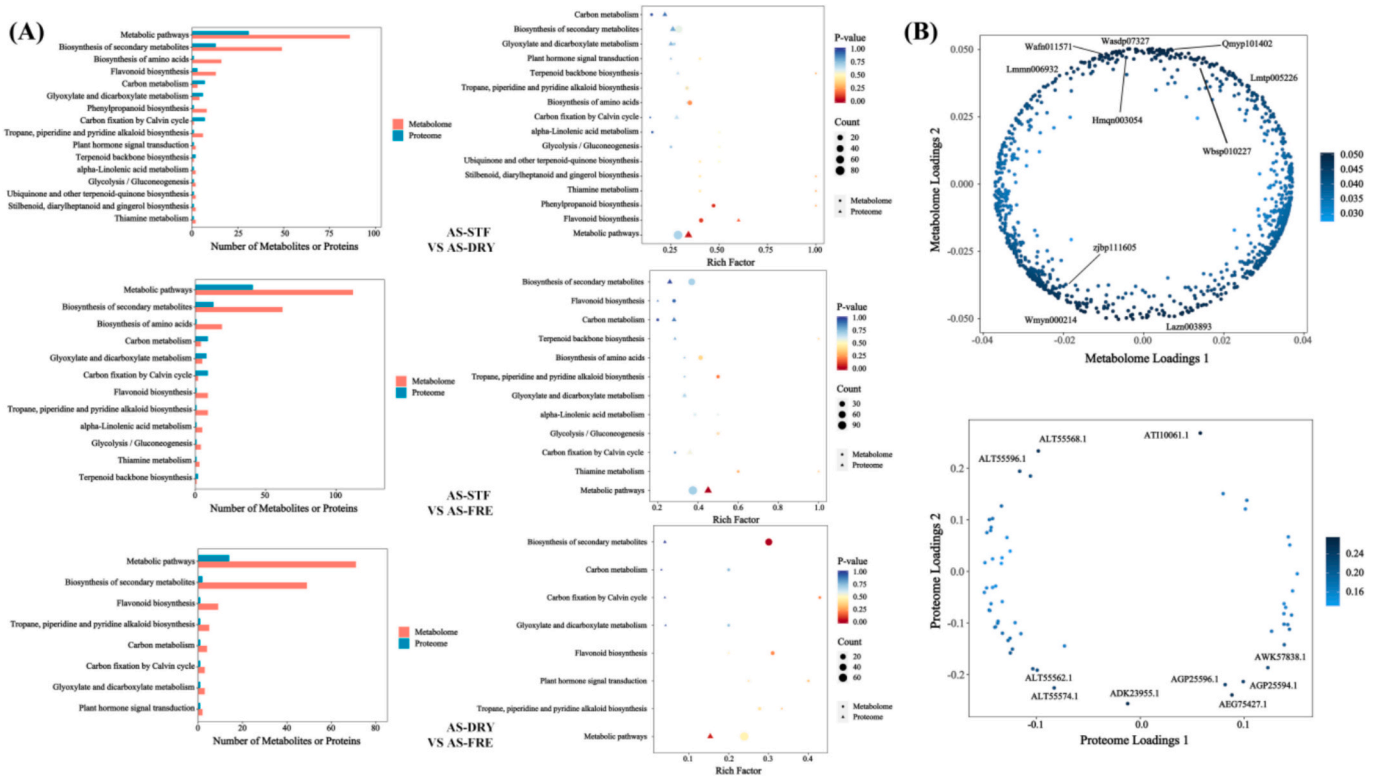

Fig. 4. Joint analysis of differential metabolites and protein expression in *Aquilaria sinensis* leaf (A: KEGG pathway enrichment analysis of differential metabolites and differential proteins; B: PCA loadings plot for metabolomics and proteomics).

Table 2
KEGG pathways involved in the differential components of *Aquilaria sinensis* leafs.

Group	No.	Description	P-values
AS-DRY VS AS-STF	1	Metabolic pathways	0.6956
	2	Flavonoid biosynthesis	0.1039
	3	Phenylpropanoid biosynthesis	0.0876
	4	Thiamine metabolism	0.4563
	5	Stilbenoid, diarylheptanoid and gingerol biosynthesis	0.4563
	6	Ubiquinone and other terpenoid-quinone biosynthesis	0.4563
	7	Glycolysis / Gluconeogenesis	0.7317
	8	alpha-Linolenic acid metabolism	0.9319
	9	Carbon fixation by Calvin cycle	0.9129
	10	Biosynthesis of amino acids	0.2379
	11	Tropane, piperidine and pyridine alkaloid biosynthesis	0.4368
	12	Terpenoid backbone biosynthesis	0.2923
	13	Plant hormone signal transduction	0.4564
	14	Glyoxylate and dicarboxylate metabolism	0.6842
	15	Biosynthesis of secondary metabolites	0.5766
	16	Carbon metabolism	0.9620
AS-FRE VS AS-STF	1	Metabolic pathways	0.7087
	2	Thiamine metabolism	0.2849
	3	Carbon fixation by Calvin cycle	0.8179
	4	Glycolysis / Gluconeogenesis	0.3622
	5	alpha-Linolenic acid metabolism	0.5960
	6	Glyoxylate and dicarboxylate metabolism	0.7410
	7	Tropane, piperidine and pyridine alkaloid biosynthesis	0.2073
	8	Biosynthesis of amino acids	0.3761
	9	Terpenoid backbone biosynthesis	0.3814
	10	Carbon metabolism	0.9787
	11	Flavonoid biosynthesis	0.9219
	12	Biosynthesis of secondary metabolites	0.6993
AS-DRY VS AS-FRE	1	Metabolic pathways	0.4749
	2	Tropane, piperidine and pyridine alkaloid biosynthesis	0.4270
	3	Plant hormone signal transduction	0.3383
	4	Flavonoid biosynthesis	0.2237
	5	Glyoxylate and dicarboxylate metabolism	0.7299
	6	Carbon fixation by Calvin cycle	0.2145
	7	Carbon metabolism	0.7372
	8	Biosynthesis of secondary metabolites	0.0100

flavonoid pathway. In addition, the enrichment of differential peroxidases suggests their dual roles in ROS scavenging and lignin polymerization, which may be associated with the antioxidant phenotype observed in AS-STF (Corpas et al., 2025; Liang et al., 2025; Wen et al., 2025).

KEGG pathway enrichment analysis between AS-STF and AS-FRE in metabolomics and proteomics also identified the biosynthesis of secondary metabolites as the most significantly enriched pathway, suggesting that stir-fried treatment markedly influenced the synthesis of secondary metabolites in *Aquilaria sinensis* leaves, particularly compounds associated with antioxidant, antibacterial, and antiviral properties. Furthermore, the biosynthesis of amino acids and flavonoid biosynthesis pathways were significantly enriched in both metabolomic and proteomic analyses, underscoring their regulatory roles during *Aquilaria sinensis* leaf processing. In proteomics, carbon metabolism also exhibited strong enrichment, reflecting the substantial impact of different processing techniques on carbohydrate metabolism in *Aquilaria sinensis* leaves. Other enriched pathways, such as glyoxylate and dicarboxylate metabolism and plant hormone signal transduction, indicated potential regulatory effects on plant growth and development. The bubble plot demonstrated that the biosynthesis of secondary metabolites and flavonoid biosynthesis pathways had low *P*-values, highlighting their significant enrichment and strong differentiation between AS-STF and AS-FRE samples.

In the comparative pathway enrichment analysis between AS-DRY and AS-FRE, metabolomic results revealed that the biosynthesis of secondary metabolites was the most enriched pathway, indicating that stir-fried significantly altered the synthesis of secondary metabolites such as flavonoids and plant hormones. Additionally, the biosynthesis of amino acids and flavonoid biosynthesis pathways were prominently enriched, suggesting their pivotal roles in metabolic differences between fresh and stir-fried samples. In proteomic analysis, carbon metabolism was a significantly enriched pathway, particularly in processes related to carbohydrate metabolism and energy transformation. Carbon fixation via the Calvin cycle and glyoxylate and dicarboxylate metabolism were also enriched in both sample groups, further elucidating the metabolic changes induced by different processing methods.

Fig. 4(B) presents the PCA loadings plots for metabolomics and proteomics (Metabolome Loadings Plot and Proteome Loadings Plot). From the metabolomics plot, it can be observed that there is a certain distribution trend among the metabolites represented by the Metabolome Loadings 1 and Metabolome Loadings 2 axes. Among them, ten metabolites, including Wafn011571, Wasdp07327, and Lmtn005226, exhibit the highest loading values, indicating their significant role in the metabolic characteristics of the samples and their potential for notable changes under specific treatments. Furthermore, the distribution pattern in the plot suggests that metabolite loadings exhibit a tendency toward aggregation or dispersion, implying that these metabolites may be influenced by different biological or processing conditions.

In the proteomics PCA loadings plot, ten proteins, including ALT55568.1, ATI10061.1, and ALT55596.1, show high loading values and are represented in dark blue, indicating their prominent role in the proteomic characteristics of the samples. Conversely, other proteins exhibit lower loading values and appear in light blue, suggesting that these proteins are relatively less significant in shaping the overall metabolic profile.

3.5. Antioxidant activity of different Aquilaria sinensis leaves

3.5.1. Toxic effects of Aquilaria sinensis leaves on HepG2 cells

The cytotoxic effects of different concentrations and processing methods of *Aquilaria sinensis* leaves on HepG2 cells were evaluated through cell viability assays. As shown in Fig. 5(A), treatment with AS-STF at concentrations ranging from 3.125 to 800 μg/mL resulted in cell viability rates between 110.29% and 134.94%, indicating a significant proliferative effect. However, at a concentration of 1600 μg/mL, cell viability decreased markedly to 53.35%, signifying substantial cytotoxicity at this level. For AS-DRY, cell viability ranged between 100.48% and 135.09% within the concentration range of 6.25 to 200 μg/mL, similarly demonstrating notable proliferative activity. When concentrations increased to 400–800 μg/mL, cell viability decreased modestly to 96.81% and 92.73%, respectively, implying no significant cytotoxic effect within this range. Nevertheless, at the highest tested concentration of 1600 μg/mL, viability dropped significantly to 44.85%, confirming a pronounced cytotoxic effect. AS-FRE exhibited clear proliferative effects within the concentration range of 12.5–800 μg/mL, with cell viability values from 100.48% to 135.09%. However, at a concentration of 1600 μg/mL, viability sharply declined to 42.14%, indicating considerable cytotoxicity at this dose. Based on these findings, concentrations of 25, 50, 100, and 200 μg/mL were selected for subsequent studies.

3.5.2. Establishment of the H_2O_2-induced cellular

H_2O_2 has strong oxidative properties and can be converted into highly reactive hydroxyl radicals within cells, triggering a series of reactions that lead to oxidative stress. As shown in Fig. 5(B), with an increase in H_2O_2 concentration, cell viability significantly decreased ($p < 0.05$). When the H_2O_2 concentration was increased from 3.125 μmol/L

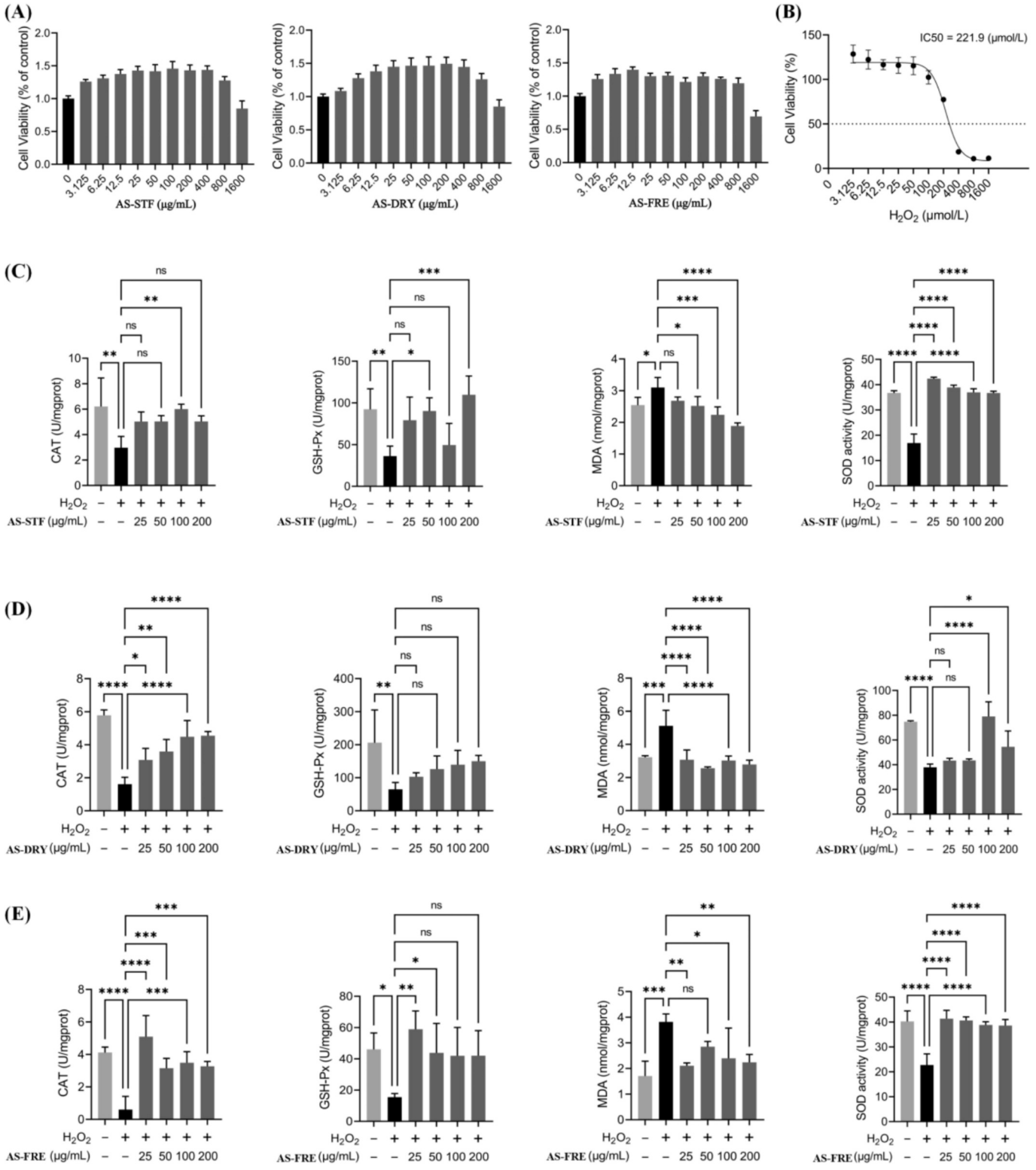

Fig. 5. The effect of *Aquilaria sinensis* leaf on antioxidant enzyme activity-related indicators in H_2O_2-induced HepG2 cells (A: Toxicity of different *Aquilaria sinensis* leaves on HepG2 cells; B: H_2O_2-induced cellular oxidative damage; C: Effect of AS-STF on antioxidant enzyme activity-related indicators in H2O2-induced HepG2 cells; D: Effect of AS-DRY on antioxidant enzyme activity-related indicators in H2O2-induced HepG2 cells; E: Effect of AS-FRE on antioxidant enzyme activity-related indicators in H2O2-induced HepG2 cells).

to 1600 μmol/L, cell viability decreased from 143.91% to 13.28%. At a concentration of 221.9 μmol/L, the cell viability was 50%. Therefore, a concentration of 200 μmol/L H_2O_2 was selected to establish the cellular oxidative damage model.

3.5.3. The effect of Aquilaria sinensis leaf on the activity of antioxidant enzymes in H2O2-induced HepG2 cells

Studies have shown that H_2O_2-induced ROS production can cause lipid peroxidation in cells, leading to the formation of MDA. Therefore,

measuring the MDA content is often used to reflect the extent of lipid peroxidation in the body and indirectly indicate the degree of cellular damage. SOD is commonly used to reflect the extent of oxidative damage in cells, as it catalyzes the dismutation of superoxide anion to generate H_2O_2 and O_2, making it the primary substance for eliminating free radicals in organisms. CAT converts the produced H_2O_2 in cells into H_2O and O_2, preventing H_2O_2 from being converted into more reactive substances, and is a key enzyme in the biological defense system. GSH is involved in redox reactions in the body, scavenging electrophilic groups, oxygen free radicals, and other substances, and exhibits strong antioxidant activity. The effects of the three types of *Aquilaria sinensis* leaves on antioxidant enzyme activity-related indicators in H_2O_2-induced HepG2 cells are shown in Fig. 5(C)**(D)(E)**.

For AS-STF, AS-FRE, and AS-DRY, compared with the blank group, the MDA content in the model group increased by 22.04%, 54.37%, and 58.70%, respectively. The activities of SOD, CAT, and GSH-PX decreased by 53.91%, 43.34%, and 49.22%, 52.10%, 30.44%, and 72.15%, and 60.70%, 66.38%, and 55.32%, indicating that lipid peroxidation occurred within the cells. After 24 h of treatment with AS-STF, the MDA content in the cells decreased in a concentration-dependent manner, and the activities of SOD, CAT, and GSH-PX were significantly higher than those in the model group. At a concentration of 200 μg/mL, the three types of *Aquilaria sinensis* leaves reduced the MDA content in cells by 39.03%, 41.36%, and 45.40% compared to the model group, while the activities of SOD, CAT, and GSH-PX increased by 116.97%, 69.64%, and 43.55%, 69.70%, 18.58%, and 181.99%, and 171.99%, 170.86%, and 131.41%, respectively. These results suggest that all three types of *Aquilaria sinensis* leaves can inhibit lipid peroxidation in HepG2 cells to some extent, providing protection against oxidative damage induced by H_2O_2. Additionally, AS-STF and AS-FRE exhibited stronger protective effects compared to AS-DRY.

4. Discussion

4.1. Differential impact of chemical composition and metabolic regulation in different Aquilaria sinensis leaves

This study systematically elucidates the significant effects of stir-fried, drying, and fresh processing on the chemical composition and metabolic pathways of *Aquilaria sinensis* leaves through comprehensive metabolomics and proteomics analyses. In terms of metabolite composition, distinct differences were observed among the three sample types regarding key components such as flavonoids, terpenoids, amino acids, and their derivatives. Specifically, AS-STF exhibited slightly higher levels of flavonoids (20.71%) and terpenoids (7.22%) compared to the AS-DRY and AS-FRE, whereas the dried sample showed a marginally higher proportion of amino acids and their derivatives (13.65%). These variations may be attributed to changes in enzyme activity or thermal effects during processing. In addition, the potential contribution of Maillard reaction products (MRPs) should be considered, especially in the stir-fried samples exposed to relatively high temperatures. During thermal processing, reducing sugars and free amino acids can undergo non-enzymatic Maillard reactions, leading to the formation of a series of newly generated compounds, including early-stage Amadori products, intermediate carbonyl compounds, and melanoidin-like end products. These compounds may partially contribute to the altered metabolic profile observed in AS-STF. Considering that amino acids and their derivatives were among the major metabolite classes detected in this study, it is plausible that part of these precursors participated in heat-induced Maillard reactions during stir-frying, thereby influencing both the abundance and composition of metabolites. The elevated temperature during stir-fried likely facilitated the synthesis or stabilization of flavonoids, while the drying process, characterized by slower dehydration, may have preserved a higher concentration of amino acid-based compounds (Liu et al., 2024).

It should also be noted that thermal processing may generate not only desirable flavor- and color-related Maillard reaction products, but also potentially hazardous heat-induced byproducts. In thermally processed foods and beverages, compounds such as acrylamide and 5-hydroxymethylfurfural (5-HMF) may be formed under roasting or toasting conditions, and their formation can be influenced by temperature, time, moisture, and precursor composition. In addition, previous studies on roasted tea products have suggested that polycyclic aromatic hydrocarbons (PAHs) may also increase depending on the heating mode and roasting intensity. Therefore, although the present results indicate that stir-fried processing enhanced the functional composition and antioxidant activity of *Aquilaria sinensis* leaves, the possible formation of process-induced hazardous compounds should not be neglected and warrants targeted safety evaluation in future studies (L. Wang et al., 2024).

In Table 3, the enriched compounds such as luteolin and its glycosides, as well as quercetin and its diglycosides, exhibit dual properties of free radical scavenging and cellular antioxidant signaling regulation. On one hand, glycosylation can significantly enhance the water solubility and stability of flavonoids, thereby improving their absorption and cellular accessibility (M et al., 2016). On the other hand, luteolin and quercetin can promote Nrf2 nuclear translocation and ARE binding, thereby inducing the expression of phase II enzymes such as HO-1, NQO1, and glutathione synthase, which in turn upregulates endogenous antioxidant and detoxification capacities. In addition, Venn diagram analysis revealed that the stir-fried sample contains 41 unique metabolites. These metabolites belong to key chemical classes, including flavonoids, terpenoids, and phenolic acids, each known for their bioactive properties. The presence of these metabolites in AS-STF is indicative of the significant metabolic changes induced by stir-frying. Specifically, flavonoids and terpenoids are often linked to antioxidant, anti-inflammatory, and antimicrobial activities, while phenolic acids play a crucial role in modulating oxidative stress and enhancing cellular defense mechanisms. These findings suggest that stir-frying not only affects the quantity but also the quality of the bioactive compounds present in *Aquilaria sinensis* leaves, contributing to its enhanced health benefits.

Proteomics data further corroborate the aforementioned findings. PCA analysis demonstrated a clear distinction between the stir-fried sample (AS-STF) and the dried sample (AS-DRY), indicating inherent differences in their protein expression profiles. Specifically, proteins such as AWK57838.1 and AWK9261.1 were significantly upregulated in the stir-fried sample, suggesting potential activation of enzymes involved in heat stress responses or secondary metabolite biosynthesis. In contrast, the protein expression within the dried sample (AS-DRY) exhibited high consistency (with a correlation coefficient approaching 1.0), implying that the natural drying process induced minimal perturbation to the proteome, likely preserving the stability of functional proteins.

KEGG pathway enrichment analysis revealed significant enrichment of pathways associated with the biosynthesis of secondary metabolites, amino acid metabolism, and flavonoid biosynthesis in both stir-fried and dried samples. For example, the enrichment of the flavonoid biosynthesis pathway is consistent with the observed increase in flavonoid accumulation in the stir-fried samples. Furthermore, notable alterations in carbon metabolism pathways, such as glyoxylate and dicarboxylate metabolism, suggest that different processing methods may influence the synthesis efficiency of secondary metabolites by modulating energy metabolism pathways (Zhang et al., 2024).

It should be noted that the KEGG enrichment results presented here were mainly used to support the biological interpretation of the multi-omics data. Although these enriched pathways provide useful clues regarding the potential metabolic regulation associated with different processing methods, no targeted validation of the specific pathways was conducted in this study. Therefore, these findings should be regarded as suggestive pathway-level associations rather than direct evidence of specific regulatory mechanisms.

Table 3
Significant differential metabolites and differential proteins in *Aquilaria sinensis* leaves.

Class	Index	Compounds	Value
Phenolic acids	Wmyn000214	Gentisic acid 5-O-β-D-(6'-O-galloyl)-gluco-pyranoside	0.0506
Lignans and Coumarins	Lazn003893	Erythro-Guaiacylglycerol-β-Coniferyl Ether	0.0506
Terpenoids	Qmyp101402	11,12-O-Isopropyfidenesolajiangxin F	0.0506
Terpenoids	Wasdp07327	β-Rotunol	0.0504
Lipids	Lmmn006932	2-Hydroxy-4-methyl-3-tridecanoyloxypentanoic acid methyl ester	0.0503
Lipids	Hmqn003054	9,10,11-Trihydroxy-12-octadecenoic acid	0.0503
Terpenoids	Lmtp005226	Santalol	0.0503
Terpenoids	Wbsp010227	3β,14α,15α,29α-tetrahydroxyserrat-14-en-3-(3′-methoxyl-4′-hydroxybenzoate)	0.0502
Terpenoids	zjbp111605	9-Hydroxyselina-3,11-dien-12-al	0.0502
Lipids	Wafn011571	α-Hydroxylinoleic acid	0.0502
Class	**Index**	**Compounds**	**Value**
Flavonoids	Zbgp007629	3′,4'-Dihydroxy-7,5′-dimethoxyflavone*	0.0501
	Lamn006359	4′-demethyl-3,9-dihydroeucomin glucoside	0.0497
	Zbbn005905	Abyssinone II	0.0496
	MWS20147	Luteolin-3'-O-glucoside	0.0495
	Hmqn003268	Dihydrotricetin	0.0492
	Cmsp006026	Dihydrorhamnetin	0.0491
	pmp000596	Quercetin-3-O-(2''-O-galactosyl)glucoside	0.0490
	Xmgp006913	2,4,2′,4′-tetrahydroxy-3′-prenylchalcone	0.0490
	MWSHY0058	Luteolin*	0.0489
	Wbtn006810	6,7-dihydroxy-1,3-dimethoxyxanthen-9-one*	0.0487
Class	**Index**	**KO**	**KEGG_map**	**Value**
Protein	ATI10061.1	K01601	ko00630,ko00710,ko01100,ko01110,ko01200	0.2742
	ADK23955.1	K02183	ko04016,ko04070,ko04075,ko04626	0.2566
	AEG75427.1	K02183	ko04016,ko04070,ko04075,ko04626	0.2553
	ALT55568.1	K02887	ko03010	0.2531
	AGP25594.1	K00487	ko00130,ko00940,ko00941,ko00945,ko01100	0.2354
	AGP25596.1	K01859	ko00941,ko01100,ko01110	0.2342
	ALT55574.1	K02707	ko00195,ko01100	0.2314
	ALT55596.1	K02982	ko03010	0.2262
	AWK57838.1	K13447	ko04016,ko04626	0.2234
	ALT55562.1	K05581	ko00190,ko01100	0.2156

These findings are consistent with previous studies, such as the high-temperature fixation process in green tea processing, which can activate polyphenol oxidase and promote the oxidative polymerization of catechin compounds (Xujiang et al., 2024). However, this study is the first to reveal the specific regulatory mechanisms of stir-fried treatment on flavonoids and terpenoid compounds in *Aquilaria sinensi* leaves, providing new insights for the optimization of its processing methods. Nevertheless, one limitation of the present study is that the contribution of Maillard reaction products was not specifically characterized. Because stir-frying involves elevated temperatures, the formation of Maillard reaction products is highly possible and may represent an important source of chemical variation beyond the regulation of endogenous biosynthetic pathways. Some of these products may also possess antioxidant or bioactive properties, thereby contributing to the functional differences among processing methods. In the present work, however, no targeted screening or structural confirmation of representative Maillard reaction markers, such as 5-hydroxymethylfurfural, furfural derivatives, advanced glycation intermediates, or melanoidin-related compounds, was performed. Therefore, the role of Maillard reaction products in shaping the overall metabolic profile of *Aquilaria sinensis* leaves requires further investigation in future studies using targeted metabolomics and complementary chemical characterization approaches.

Furthermore, the 2-h boiling reflux used in this study is a critical step for extracting bioactive compounds from *Aquilaria sinensis* leaves. However, we acknowledge that this prolonged exposure to high temperature is a potential cause for the degradation of heat-sensitive metabolites. Specifically, polyphenols, flavonoids, and terpenoids, which are known for their antioxidant properties, are susceptible to thermal degradation. Prolonged boiling could result in the breakdown of these compounds, reducing their bioactivity and stability. The degradation of these metabolites could have been particularly impactful on the overall chemical composition of the sample, and it is likely that the metabolite profile would have been altered during this process. The high temperature during the boiling reflux may have contributed not only to the breakdown of thermally unstable compounds, but also to the generation of heat-induced reaction products, including potential Maillard reaction products formed from reducing sugars and amino acids. Therefore, some of the observed differences in metabolite concentrations across the processed samples may reflect the combined effects of metabolite degradation, transformation, and de novo formation of thermal reaction products.

Future studies are needed to investigate the impact of extended boiling times on the stability of such compounds and to explore potential modifications in processing methods that could minimize the degradation of these sensitive metabolites while still achieving effective extraction. This would help to optimize the balance between maximizing bioactive compound yield and preserving their functional properties during processing.

4.2. Integrated metabolomics and proteomics analysis and regulatory network of Aquilaria sinensis leaves

This study integrated metabolomics and proteomics data to construct a metabolic regulatory network for different *Aquilaria sinensis* leaves. Metabolomics data showed that the number of differential metabolites in the stir-fried sample was significantly higher than in other groups (e.g., 797 upregulated metabolites in AS-STF vs. AS-DRY), with flavonoids (e.g., Luteolin-3'-O-glucoside) and phenolic acids (e.g., Gentisic acid derivatives) being enriched in the stir-fried sample. Proteomics analysis revealed that the expression levels of secondary metabolism-related enzymes (e.g., P450 monooxygenase) and stress response proteins (e.g., heat shock proteins) were significantly elevated in the stir-fried sample. The integrated analysis of both datasets indicated a strong

correlation between metabolite accumulation and protein expression changes. For instance, the synthesis of flavonoids may be driven by the upregulation of phenylalanine ammonia-lyase (PAL) and chalcone synthase (CHS)(Kaur et al., 2025); in the proteomics data; the PAL homolog protein (e.g.; AMQ67166.1) was highly expressed in AS-STF; directly supporting this mechanism. Furthermore; the enrichment of the glyoxylate and dicarboxylate metabolism pathway (Rich Factor = 0.32; P = 0.002) suggests that stir-fried may influence the production of antioxidant precursors (e.g.; glycine) by regulating the photorespiration pathway. This cross-omics association provides new insights for deciphering complex metabolic networks (Surat et al., 2023).

From a methodological standpoint, the key metabolites (e.g., Wafn011571) and proteins (e.g., ALT55568.1) identified through PCA loadings analysis represent potential targets for subsequent functional investigations. For instance, Wafn011571 (α-Hydroxylinoleic acid) may mitigate inflammation by inhibiting the NF-κB signaling pathway (Sheng-Nan et al., 2023); while ALT55568.1 could be involved in the post-translational modification of ROS scavenging enzymes. Furthermore; KEGG pathway enrichment analysis provided additional insights into cross-omics regulatory hubs. The biosynthesis of secondary metabolites was significantly enriched in both metabolomics and proteomics data (Rich Factor > 5; $P < 0.01$); underscoring this pathway as a central target of the observed effects. Notably; the enrichment of carbon metabolism pathways suggests a coupling between energy supply and secondary metabolism: stir-fried may enhance glycolysis or the tricarboxylic acid cycle; thus providing ATP and carbon skeletons essential for secondary metabolite biosynthesis; thereby promoting the synthesis of flavonoids and terpenoids (Gong et al., 2025), This mechanism parallels the high-temperature-induced catechin synthesis observed in tea plants, but this study represents the first to establish a comprehensive regulatory network linking metabolites, proteins, and pathways in *Aquilaria sinensis* leaves.

To further explore the regulatory relationship between protein expression and metabolite accumulation, this study conducted a preliminary co-expression correlation analysis. Using Pearson correlation and hierarchical clustering, key differentially expressed proteins (DEPs) were mapped against differential metabolites. To reduce the likelihood of false-positive associations caused by multiple testing, the significance of the correlations was further evaluated using Benjamini-Hochberg false discovery rate (FDR) correction, and only correlations meeting the predefined significance criteria after adjustment were considered for interpretation. The results revealed strong positive correlations between certain flavonoid biosynthetic enzymes (e.g., AMQ67166.1, homologous to PAL) and specific flavonoids (e.g., Luteolin-3'-O-glucoside, Wafn011571), with correlation coefficients exceeding 0.85. This suggests that the expression of upstream biosynthetic enzymes directly contributes to the accumulation of downstream flavonoid compounds. Additionally, proteins such as ALT55568.1 and AWK57838.1 showed significant co-expression with terpenoid and phenolic acid metabolites, indicating their potential regulatory roles in secondary metabolism.

Based on the correlation matrix, a preliminary multi-omics regulatory network was constructed. This network highlights several potential regulatory modules, including PAL-Luteolin-3'-O-glucoside and ALT55568.1-α-Hydroxylinoleic acid interactions. Such modules suggest that stir-fried treatment activates not only biosynthetic pathways but also triggers coordinated expression of enzymatic machinery and metabolite production. In addition, to improve the robustness of the correlation-based network, multiple testing correction using the Benjamini-Hochberg false discovery rate (FDR) method was incorporated into the correlation analysis, thereby reducing the risk of false-positive associations in the large-scale multi-omics dataset. While this network remains exploratory, it provides a foundation for future targeted validation using gene knockout or enzyme activity assays. The integration of such regulatory networks enhances the biological interpretability of omics data and helps uncover functional nodes within complex metabolic systems.

Although the proteomics analysis identified key differentially expressed proteins (e.g., PAL, CHS, ALT55568.1) that potentially regulate antioxidant metabolite accumulation, we acknowledge that these findings have not yet been verified by targeted validation methods such as Western blotting (WB) or ELISA. As this study was designed as a discovery-oriented investigation, our primary goal was to uncover candidate proteins and pathways using high-throughput omics approaches. Due to current limitations in experimental resources and manuscript scope, we were unable to validate all differentially expressed proteins individually. Nevertheless, we applied stringent statistical thresholds, used technical replicates, and integrated proteomic and metabolomic datasets to ensure data reliability. The strong internal consistency—such as the co-occurrence of PAL upregulation with flavonoid enrichment—further supports the credibility of the results. In future studies, we plan to validate key protein targets such as PAL and CHS through WB or ELISA to confirm their regulatory roles in secondary metabolism and antioxidant response.

4.3. Antioxidant activity of Aquilaria sinensis leaf and potential for functional development

Antioxidant assays demonstrated that all three types of *Aquilaria sinensis* leaves effectively mitigated H_2O_2-induced oxidative damage in HepG2 cells, with the AS-STF and AS-FRE exhibiting significantly superior protective effects compared to the AS-DRY. At a concentration of 200 μg/mL, the AS-STF reduced MDA levels by 39.03%, and significantly increased the activities of SOD, CAT, and GSH-PX by 116.97%, 69.70%, and 171.99%, respectively, compared to 45.40%, 43.55%, and 131.41% in the AS-DRY. These findings are strongly consistent with metabolomics data, where the enrichment of flavonoids (e.g., Luteolin) and phenolic acids (e.g., Gentisic acid derivatives) in the AS-STF likely enhances antioxidant capacity through mechanisms such as free radical scavenging and metal ion chelation (Hadeil & Ulfat, 2017; Na et al., 2023). Additionally, the stir-fried process may facilitate the release of certain lipophilic antioxidant compounds (e.g., terpenoids), thereby improving their bioavailability.

Notably, the increased activities of SOD, CAT, and GSH-PX in the AS-STF group may also be mechanistically linked to the activation of the Nrf2/ARE signaling pathway. Several flavonoids and phenolic acids enriched in the stir-fried sample, such as luteolin, have been reported to upregulate antioxidant enzyme expression by promoting the nuclear translocation of Nrf2, a key transcription factor regulating cellular oxidative stress responses. Upon activation, Nrf2 binds to the antioxidant response element (ARE) in the promoter regions of target genes, leading to enhanced transcription of detoxifying and antioxidant enzymes including SOD, CAT, and GSH-PX. Therefore, the superior antioxidant performance of the stir-fried sample may not only stem from direct radical scavenging by metabolites, but also from indirect regulation of cellular antioxidant defense systems via Nrf2-mediated gene expression. However, it should be noted that the involvement of the Nrf2/ARE signaling pathway in the observed antioxidant effects remains hypothetical at this stage, and further molecular or genetic validation is required to confirm its functional role.

Moreover, our proteomic data showed that key enzymes involved in flavonoid and phenolic acid biosynthesis, such as phenylalanine ammonia-lyase (PAL), were significantly upregulated in the AS-STF group, supporting enhanced metabolic flux toward antioxidant compound synthesis. These findings complement the metabolomics results and provide a mechanistic explanation for the observed increase in antioxidant enzyme activity in HepG2 cells. Although enzymes such as SOD and GSH-PX are not expressed in plant tissue and were thus not detected in our leaf proteome datasets, the upregulation of secondary metabolite synthesis in AS-STF samples likely triggered antioxidant defense responses in cells. In this context, the increased intracellular antioxidant enzyme activity observed in the cellular assays reflects a downstream biological effect of the enhanced metabolite profile induced

by the stir-fried treatment.

However, at high concentrations (1600 μg/mL), *Aquilaria sinensis* leaf extract exhibited cytotoxic effects, reducing cell viability to approximately 50%. This dual effect highlights the need to balance the enrichment of active metabolites with the control of potential toxicity during processing. For example, optimizing stir-fried conditions, including temperature and time, could enhance the retention of beneficial metabolites (such as flavonoids) while minimizing the formation of potentially harmful compounds (such as certain alkaloids). Moreover, the relatively lower antioxidant activity observed in the dried samples may be attributed to the loss of heat-sensitive components, such as vitamin C (Negi et al., 2025).

4.4. Sustainable development and environmentally friendly green strategies for Aquilaria sinensis leaf

Aquilaria sinensis leaves, as a by-product of the agarwood tree (*Aquilaria sinensis*), offer an efficient means of utilization that aligns with the principles of circular economy and sustainable development. This section builds on the core findings of the study by exploring how insights from the stir-frying process can inform greener, more efficient processing strategies for maximizing the value of *Aquilaria sinensis* leaves. The traditional *Aquilaria sinensis* industry, which predominantly focuses on the exploitation of agarwood, has resulted in the underutilization of leaves. However, studies have demonstrated that *Aquilaria sinensis* leaves are rich in bioactive compounds such as flavonoids, terpenoids, and phenolic acids, which exhibit notable antioxidant, anti-inflammatory, and antimicrobial properties (Jiang, Mou, et al., 2024). For instance, flavonoids can enhance cellular antioxidant capacity by scavenging free radicals and modulating the Nrf2/ARE signaling pathway, while terpenoids like β-Rotunol have been shown to inhibit lipid peroxidation. Consequently, agarwood leaves hold potential for development into functional beverages, natural food preservatives, or pharmaceutical raw materials, providing a sustainable alternative to synthetic additives and reducing both environmental and health risks.

For practical applications, standardized extracts of *Aquilaria sinensis* leaves can be prioritized in two main directions. The first is skin antioxidant applications (e.g., repairing serums, facial masks, after-sun recovery lotions). Based on the observed flavonoid enrichment and cellular antioxidant phenotype, flavonoids and their glycosides can serve as the main functional agents. Their activity can be preserved through mild thermal processing and low-oxygen/light-avoiding conditions, while delivery systems such as aqueous solubilization enhancement and liposomes can further improve skin penetration and stability. The second is plant-based functional beverages targeting populations with high oxidative stress. Representative marker compounds (e.g., luteolin and its glycosides, quercetin derivatives) should be subjected to targeted quantification to establish a quality control framework ensuring batch-to-batch consistency.

In this study, significant protective effects on HepG2 cells were observed within functionally relevant dose ranges, but cytotoxic signals emerged at extremely high concentrations. Therefore, during industrial translation, development should be guided by the intended dosage range, with stepwise completion of in vitro safety screenings, necessary in vivo safety and intake evaluations, and assessments of population suitability. At the same time, physicochemical and microbiological limits, impurity control, and adverse reaction monitoring for both raw materials and finished products should be incorporated. These measures will ensure the effective translation of laboratory evidence into skincare formulations and functional beverages.

In terms of green processing technologies, the high energy consumption and carbon emissions associated with traditional stir-fried methods require optimization. Studies suggest that integrating solar drying technology with intelligent temperature control systems can reduce energy consumption by 30%–50% (Xu & Liu, 2025); while microwave-assisted heating; which selectively heats based on molecular polarity; not only reduces drying time by 40% but also helps preserve heat-sensitive components such as vitamin C and polyphenols (Xu & Liu, 2025). In terms of environmental benefits, solar drying has been shown to reduce approximately 180–250 kg CO_2-equivalent emissions per ton of dried leaves compared to conventional hot-air drying.

This biochar significantly enhances soil water retention and nutrient adsorption capacity (Tu et al., 2025). Furthermore; the fiber and polysaccharide components of the residue can be utilized as feed additives for ruminants; and upon microbial fermentation; short-chain fatty acids (SCFAs) can be produced; contributing to increased Omega-3 content in dairy products (Pasta et al., 2023), This process enables the conversion of "waste" into high-value products.

5. Conclusion

This study integrates metabolomics, proteomics, and cellular assays to comprehensively elucidate the unique advantages of stir-fried treatment on the chemical composition and bioactivity of *Aquilaria sinensis* leaves. The stir-fried process, through high-temperature-induced chemical reactions (such as flavonoid stabilization and terpenoid enrichment), significantly enhanced both the diversity and concentration of secondary metabolites in *Aquilaria sinensis* leaves, particularly the accumulation of flavonoids and phenolic acids. Proteomic analysis further highlighted the pivotal regulatory role of stir-fried in secondary metabolic pathways, including the upregulation of carbon metabolism and key enzymes involved in flavonoid biosynthesis, thereby providing adequate carbon skeletons and energy for metabolite synthesis. Antioxidant activity assays demonstrated that the AS-STF exhibited superior radical scavenging capacity at the cellular level, likely mediated by the activation of the Nrf2/ARE signaling pathway and the synergistic enhancement of antioxidant enzymes (SOD, CAT). Compared to the AS-DRY and AS-FRE, AS-STF showed distinct advantages in retaining functional components and enhancing bioactivity. Nevertheless, the improved functional performance observed in the stir-fried samples should be interpreted together with potential processing-related safety considerations. Because the present study did not quantify hazardous thermal byproducts, such as acrylamide, 5-HMF, or PAHs, a comprehensive evaluation of stir-fried *Aquilaria sinensis* leaves should combine both bioactivity assessment and contaminant monitoring in future work.

Specifically, the flavonoid and phenolic acid-enriched AS-STF extract can be further developed into high-end functional beverages (e.g., antioxidant herbal teas), natural antioxidant additives in food preservation, and plant-derived skincare or cosmeceutical products. In particular, its Nrf2/ARE-mediated cellular antioxidant potential suggests promising application in anti-aging and oxidative stress-related formulations. Overall, these findings reinforce the importance of processing optimization in enhancing both the nutritional and functional properties of *Aquilaria sinensis* leaves. Future investigations should focus on the dynamic effects of stir-fried on specific metabolite-protein interaction networks and explore its potential applications in anti-inflammatory, antimicrobial, and other therapeutic areas.

CRediT authorship contribution statement

Zixiao Jiang: Writing – original draft, Methodology, Formal analysis, Data curation, Conceptualization. **Haoji Liang:** Writing – original draft, Validation, Software, Resources, Data curation. **Dandan Chen:** Software, Formal analysis. **Yaohua Huang:** Writing – original draft, Supervision. **Nie Li:** Visualization, Supervision, Investigation. **Yiqi Wang:** Visualization, Resources. **Yangyang Liu:** Writing – review & editing, Project administration, Conceptualization.

Informed consent statement

Not applicable.

Funding

This study is sponsored by the Hainan Province Science and Technology Special Fund (Grant No.: ZDYF2025SXLH015); Hainan Outstanding Talent Team Project, China (Grant No.: HNYT20240003); Hainan Provincial Natural Science Foundation of China (Grant No.: 325QN472); International Science & Technology Cooperation Program of Hainan Province (Grant No.: GHYF2026011).

Declaration of competing interest

The authors declare that they have no known competing financial interests or personal relationships that could have appeared to influence the work reported in this paper.

Appendix A. Supplementary data

Supplementary data to this article can be found online at https://doi.org/10.1016/j.fochx.2026.103808.

Data availability

Data will be made available on request.

References

Ahmed, I. A. M., Juhaimi, F. Y. A., Özcan, M. M., Uslu, N., & Karrar, E. (2024). The effects of different cooking systems on changes in the bioactive compounds, polyphenol profiles, biogenic elements, and protein contents of cauliflower florets. *Processes, 12*(10), 2114.

Corpas, F. J., Gordo, S. G., Vargas, M. A. M., Ruiz, M. R., Torres, C. R., & Palma, J. M. (2025). Endogenous NO fluctuations in arabidopsis leaves influence peroxisomal activities and ROS, NADPH, and H2S metabolism. *Plant Science : An International Journal of Experimental Plant Biology*, Article 112683.

Demichev, V., Messner, C. B., Vernardis, S. I., Lilley, K. S., & Ralser, M. (2020). DIA-NN: Neural networks and interference correction enable deep proteome coverage in high throughput. *Nature Methods, 17*(1), 41–44.

Feng, J., Chen, W., Dong, M., & Xu, T. (2012). Study on the extraction of total proteins of semen aesculi and its dynamic changes. Chinese Herbal Medicine, 43(06), 1174–1177.

Fonseca, D., Martins, N., Garcia, R., & Cabrita, M. J. (2025). The potential of enzymatic hydrolysis with HS-SPME-GC×GC-ToFMS for the study of volatile signature of grapes. *LWT, 215*, Article 117314.

Gong, Q., Wang, J., Zhao, W., Liu, J., Yang, S., Gao, Y., … Sun, H. (2025). Development of fast-growing chlorophyll-deficient chlorella pyrenoidosa mutant using atmospheric and room temperature plasma mutagenesis. *Bioresource Technology*, Article 132245.

Guo, A., & Jia, W. (2025). Metabolomics and proteomics analysis elucidate the regulation of selenium uptake and metabolism by selenite via glutathione s-transferase in fermented goat milk. *Food Chemistry, 491*, Article 145328.

Haas, B. J., Papanicolaou, A., Yassour, M., Grabherr, M., Blood, P. D., Bowden, J., … Regev, A. (2013). De novo transcript sequence reconstruction from RNA-seq using the trinity platform for reference generation and analysis. *Nature Protocols, 8*(8), 1494–1512.

Hadeil, M. A., & Ulfat, M. O. (2017). A comparative study to evaluate the polyphenol content and antioxidant activity of coffee with fresh whole milk and evaporated milk. *Food and Public Health, 7*(4), Article 6.

Jeon, J. E., Kim, J.-G., Fischer, C. R., Mehta, N., Dufour-Schroif, C., Wemmer, K., Mudgett, M. B., & Sattely, E. (2020). A pathogen-responsive gene cluster for highly modified fatty acids in tomato. Cell, 180(1), 176–187.e119.

Ji, Z., Liu, R., & Fan, Z. (2024). Preparation and antioxidant activity of polysaccharides from artemisia capillaris buds. *Chinese Journal of Food, 24*(04), 235–246.

Jiang, Z., Hou, W., Feng, J., Zhang, S., Wang, M., & Liu, Y. (2024). Optimized green extraction of agarwood essential oil using custom natural deep eutectic solvents: Chemical analysis and bioactivity evaluation. *LWT, 214*, Article 117125.

Jiang, Z., Mou, J., Feng, J., Zhang, S., Li, D., & Liu, Y. (2024). Comparative analysis of volatile components in Chi-Nan and ordinary agarwood aromatherapies: Implications for sleep improvement. *Pharmaceuticals (Basel, Switzerland), 17*(9), 1196.

Joardder, M. U. H., & Karim, M. A. (2025). Toward uniform microwave heating in food drying: Principles, technologies, and emerging trends. Food Engineering Reviews (prepublish), 1–20.

Kaur, G., Oberoi, H. K., Kaur, M., & Umakanth, A. V. (2025). Redox metabolism stimulation in bioethanol *Sorghum* under water deficit stress. Sugar Tech (prepublish), 1–14.

Liang, C., Lin, L., Wang, X., & Zhu, W. (2025). The secretion of pseudomonas unconventional peroxidase facilitates extracellular carbon acquisition from heterogeneous lignin. *Communications Biology, 8*(1), 1318.

Liu, L., Bi, J., Chi, Y., & Chi, Y. (2024). Effects of pasteurization temperature and amino acids on the gelation behavior of liquid egg yolk: Emphasizing rheology, gel properties, intermolecular forces and microstructure. *Food Chemistry, 463*(Pt 4), Article 141508.

Liu, W., Ding, H., Li, M., & Lv, S. (2021). Research progress and development and utilisation of agarwood leaves. *Guangdong chemical industry, 48*(24), 79–80.

M, K. B., Sanae, E., Rahel, B., Petre, D., Markus, G., Laurent, B., … Christoph, R. (2016). 7-rhamnosylated flavonols modulate homeostasis of the plant hormone auxin and affect plant development. *The Journal of Biological Chemistry, 291*(10), 5385–5395.

Mu, W., Zhao, Y., Wang, Z., He, Y., Yang, C., & Wang, J. (2024). Combining lipase enzymatic techniques and antioxidants on the flavor of structured lipids (SLs) prepared from goat butter and coconut oil. *Food Bioscience, 60*, Article 104332-.

Na, L., CaiPing, W., HongTao, Z., ChangJie, G., HaoYan, Z., & DaYong, R. (2023). 1-Methylcyclopropene alleviates postharvest chilling injury of snap beans by enhancing antioxidant defense system. *Food Technology and Biotechnology, 61*(3), 283–293.

Negi, A., Infant, V., & Moses, J. A. (2025). Effect of drying techniques, conditions and feed types on the quality of dried curry leaf powder. *Food Chemistry, 463*(P2), Article 141268.

Niyigaba, T., Küçükgöz, K., Krajewska, D. K., Królikowski, T., & Trząskowska, M. (2025). Advances in fermentation technology: A focus on health and safety. *Applied Sciences, 15*(6), 3001.

Pasta, C., Caccamo, M., Petriglieri, R., Difalco, A., Farina, G., Belvedere, G., … Alcaine, S. D. (2023). Sicilian whey: Utilization of ricotta whey in the production of value-added artisanal beers. *Fermentation, 10*(1).

Sheng-Nan, Y., Mu-xuan, W., Jin-Long, H., Cai-Yun, F., Meng, W., Min, W., … Chao, L. (2023). Improved colonic inflammation by nervonic acid via inhibition of NF-κB signaling pathway of DSS-induced colitis mice. *Phytomedicine, 112*, Article 154702–154702.

Suguru, N., Naoyoshi, N., Yuya, K., Yasushi, K., Tohru, M. A., Moto, K., … Masahira, H. (2022). Extensive gut virome variation and its associations with host and environmental factors in a population-level cohort. *Nature Communications, 13*(1), 5252.

Surat, D., Simran, B., & Anita, L. (2023). Addressing ozone pollution to promote united nations sustainable development goal 2: Ensuring global food security. *Chemosphere, 347*, Article 140693.

Tang, L. (2020). *Study on the extraction and in vitro antioxidant and hypolipidemic activity of red raspberry seed oil*.

Tu, J., Mao, T., Xie, S., Xiao, H., & Wang, P. (2025). Dual chemical crosslinking strategy to fabricate lightweight, flame-retardant, high-modulus and hydrophobic cellulose cryogel. *Carbohydrate Polymers, 355*, Article 123364.

Wang, L., Wen, M., Zhou, Y., & Zhang, L. (2024). The variation of acrylamide and 5-hydroxymethylfurfural in tea with different roasting degrees and the effects of tea polyphenols on their formation. *Journal of the Science of Food and Agriculture, 104*(15), 9379–9389.

Wang, S., Xie, Y., Jin, Y., Zhou, Z., & Liu, L. (2024). Studies on the analgesic and anti-inflammatory effects of agarwood leaves. *Journal of Yunnan University for Nationalities (Natural Science Edition), 33*(01), 17–22.

Wen, J., Liu, S., Yang, B., Tan, M., Shen, X., & Du, Z. (2025). Peroxiredoxin 4 (prx 4) plays important gene expression regulatory roles in antimicrobial innate immune by regulating hydrogen peroxide (H_2O_2) in the hepatopancreas of freshwater crayfish *procambarus clarkii*. *Developmental and Comparative Immunology*, Article 105438.

Xiaowen, C., Shan, D., Wenliang, B., Yan, D., Ruijuan, G., Fuguo, L., … Xuebo, L. (2021). Methylated metabolites of chicoric acid ameliorate hydrogen peroxide (H2O2)-induced oxidative stress in HepG2 cells. *Journal of Agricultural and Food Chemistry, 69*(7), 2179–2189.

Xu, G., & Liu, H. (2025). Efficiency analysis of solar drying system integrated with flat-plate solar collector and thermal storage units. *Renewable Energy, 243*, Article 122569.

Xujiang, S., Yuliang, D., Linchi, N., Le, C., Shan, Z., Yongwen, J., … Jia, L. (2024). The influence of fixation temperature on Longjing tea taste profile and the underlying non-volatile metabolites changes unraveled by combined analyses of metabolomics and e-tongue. *LWT, 191*, Article 115560.

Zhang, Y., Dong, W., Ma, H., Zhao, C., Ma, F., Wang, Y., … Jin, M. (2024). Comparative transcriptome and coexpression network analysis revealed the regulatory mechanism of astragalus cicer l. in response to salt stress. *BMC Plant Biology, 24*(1), 817.

Zhiqiang, P., Xinyu, M., Shaoqun, Z., Sheng, Y., Guizhou, L., Chengkai, L., Jinpeng, W., Lingfei, H., & Peng, X. (2023). Microbiota-mediated nitrogen fixation and microhabitat homeostasis in aerial root-mucilage. *Microbiome, 11*(1), 85.